Inorganica Chimica Acta, 57 (1982) 171–193
©Elsevier Sequoia S.A., Lausanne – Printed in Switzerland

On the Absolute Configuration of Organometallic Compounds. X.* A Comparison of Structures for Racemic $(\eta^5\text{-}C_5H_5)Mo(CO)_2SC(CH_3)N\text{-}[CH(C_2H_5)C_6H_5]$ and $(+)_{579}\text{-}(\eta^5\text{-}C_5H_5)Mo(CO)_2SC(\alpha\text{-}C_{10}H_7)N[(S)\text{-}CH(CH_3)C_6H_5]$

MICHAEL CRESWICK and IVAN BERNAL
Chemistry Department, University of Houston, Houston, Tex. 77004, U.S.A.

Received May 29, 1981

The crystal and molecular structures of two compounds of composition $(\eta^5\text{-}C_5H_5)Mo(CO_2SC(R)N\text{-}(R')$ *were determined by X-ray diffraction (MoKα) measurements carried out at room temperature. Compound (I), the racemic compound, with* $R = CH_3$ *and* $R' = CH(C_2H_5)C_6H_5$*, crystallizes in space group* $P\bar{1}$ *(Z = 2) and cell parameters:* a = *9.264(2),* b = *9.350(2),* c = *12.592(5) Å, α = 76.24(3), β = 77.11(3) and γ = 58.83(2)°; V = 899.84 Å³. A refinement of 284 parameters, using 3415 observed* $[I > 2\sigma(I)]$*, gave the conventional agreement factors R = 0.028 and* R_w *= 0.035. The two enantiomers in the unit cell are assigned chirality indicators (*vide infra*) of (*S*; Mo)(*S*; C) and (*R*; Mo)(*R*; C). Compound (II), an optically pure diastereoisomer characterized by a (+) rotational strength at 578 nm, has* $R = \alpha\text{-}C_{10}H_7$*-(naphthyl) and* $R' = (S)\text{-}CH(CH_3)C_6H_5$*. It crystallizes in the space group* $P2_12_12_1$ *(Z = 4) with* a = *10.028(3),* b = *12.532(7) and* c = *17.774(6) Å; V = 2236.46 Å³. Refinement (171 variables using 3160 reflections having* $I > 2\sigma(I)$*) gave R = 0.018 and* R_w *= 0.019. The absolute configuration, determined by the Bijvoet method, assigns chirality indicators of (*R*; Mo)(*S*; C) to the two sites of this,* non-preferred, *diastereoisomer.*

Concerning the series of $CPMo(CO)_2$(thioamide) compounds studied here, the following conclusions can be drawn: (a) the $CpMo(CO)_2SCN$ fragments of the three species described here, and three more published earlier, display nearly identical geometrical parameters despite the changes in the nature, and bulk, of the substituents R and R′ (b) variations in the Mo–S and Mo–N are noted which are inversely correlated; *i.e.*, as the Mo–S bond increases, the Mo–N bond decreases. These small changes had been noted earlier and are further documented with these determinations (c) the torsional arrangement of the Cp ring carbons with respect to the atoms in the basal plane (*i.e.*, two *cis*-CO's and S and N, in this case) was noted to, *consistently*, display a Cp carbon staggered between the two carbonyls. This is true not only for the six $CpMo(CO)_2$(thioamide) compounds studied in this group but was found to extend to *eighteen* compounds available in the literature sharing the common 'four-legged piano stool' 'square-pyramidal' geometry. Inspite the fact that these substances crystallize in different systems and in a variety of space groups, thus being subject to totally different packing forces, there is a Cp carbon staggered between the two *cis* basal plane carbonyls whenever *Hetero Atoms* (S, N, P, Cl, *etc.*) occupy one or more of the two positions adjacent to the carbonyls. *Deviations from this rule are minor and described in the text.* As a consequence of the staggering with respect to the CO's, one of the Cp carbons is, invariably, directly, (or nearly so) above one of the hetero atoms. In the text, a description is given of which hetero atom is chosen by the Cp carbons whenever there is a competition between two *cis* hetero atoms, such as P and Cl. There is no relationship between the nature of the hetero atom chosen by the eclipsing carbon and the value of the OC- -M- -L *trans* angles. Finally, since *very bulky* groups are frequently eclipsed by a Cp carbon (*i.e.*, P of triphenylphosphine) internal steric interactions seem to have little effect on this phenomenon. However, there is an inverse correlation between the *trans* influence exerted by a basal plane ligand and the probability of its being eclipsed by the Cp carbon. (d) for the *preferred diastereoisomers* studied earlier, the plane of the phenyl ring on the optically active group $[-CH(CH_3)(C_6H_5)]$, invariably present in all these systems, faces the edge of the Cp ring. This is equally true of the two preferred diastereoisomers (constituting the enantiomeric pair of compound (I)) described here. However, compound (II) is a *non-preferred* diastereoisomer; in fact, the first of its kind reported thus far. For this substance, the chirality at the Mo site is opposite all others we have studied *and*, in this case, the phenyl ring sits as far away as possible from the Cp ring.

---

*For contribution No. IX, see ref. 5 of this paper.

Introduction

In a previous paper [1], we established the relationship between the absolute configuration at the Mo site and the sign of rotational amplitude at 589 nm for compounds of the type *1*:

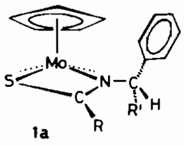
1a

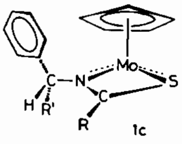
1c

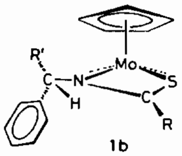
1b

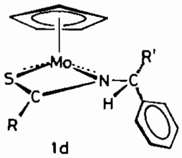
1d

From the work of Brunner *et al.* [2] it was already known that the equilibrium ratio between diastereomers *1a* and *1b* is strongly influenced by the nature of groups R and R′ on the thioamide precursor. The following diastereomeric ratios have been determined by Brunner and his associates for compounds of the type *1*, with various R and R′ substituents:

R′	R=H	CH_3	C_6H_5	α-$C_{10}H_7$
CH_3	50:50	69:31	77:23	87:13
C_2H_5	50:50	89:11	95:5	–
i-C_3H_7	50:50	98:2	99:1	–

In our earlier paper [1] we established for the compound with R = CH_3, prepared from (*S*)-α-phenylethyl amine, that the preferred (P) diastereomer has the absolute configuration shown in *1a*. According to the rules of nomenclature we suggested previously [3, 4], such a configuration at the Mo site would be assigned the symbol (*S*). Having then only one example, and unable to comment very much on the subject of conformation, we confined ourselves to a presentation of structural data and to a comparison of our stereochemical results with those of related compounds available in the published literature. In a recent report [5], we presented a number of interesting, general observations relating to conformational preferences of compounds in the Mo–thioamide series. The conclusions derived from our most recent papers can be summarized as follows:

a) The band at 589 nm, which has a low (~10^2) extinction coefficient [9, 10] and which is probably due to transitions involving, largely, metal-centered orbitals, always has a negative rotational strength for thioamides having an (*S*) absolute configuration *at the metal*. This relationship holds, regardless of the nature of groups R and R′ and regardless of the chirality of amine chosen. Thus, the sign of rotation at 589 nm may be used, for compounds of type *1*, as a diagnostic in determining the absolute configuration at Mo.

b) Since each compound has two chiral centers, synthesis using a racemic amine should yield four diastereomers (*1a–d*), whose relative abundance will reflect the stereospecificity of the overall synthesis. As indicated in the preceding table, four diastereoisomers are produced, with one enantiomeric pair preferred over the other, so long as R is bulkier than hydrogen.

c) Additionally, the conformation of the preferred diastereomer, whether arising from a racemic or an optically pure ligand, is ALWAYS one in which the plane of the phenyl ring, (substituted β to Mo) faces the edge of the Cp ring. This might, at first, appear to be a solid state effect; however, as reported before, five separate structural investigations show that independent of space group and that independent of whether packing involves pairs of enantiomers, optically pure diastereomers, *etc.*., *the preferred c*onformation has its phenyl and Cp rings oriented as shown in *1a*.

d) All of our structural investigations of racemic mixtures, thus far, have been of the preferred pairs. We now know that for (*S*; C) we get (*S*; Mo) and for (*R*; C) we get (*R*; Mo); however, since the two sites are connected by flexible single bonds, it is not, *per se*, necessary that the pair of isomers having opposite chiralities at their optical centers have to be true *Mirror Images* of one another; the two may have different *Conformations*, while still possessing antipodally related centers. Crystallographically speaking, there are two ways in which the preferred enantiomeric pair, derived from a racemic amine, may pack in the unit cell: (1) the pair may be truly *Enantiomeric*, in which case the two molecules are related by an operation of the second sort (usually a mirror plane or inversion center); (2) the pair, though antipodally related in their chiral *centers*, may be unrelated in their overall conformations, and may pack in a non-centrosymmetric space group, with two crystallographically independent molecules in the asymetric unit. It is interesting to note that although we have found two cases (one Mo–thioamide [5] and one other optically active Mo [6a] complex) of pure diastereomers to pack according to scheme (2); all racemic mixtures we have examined, thus far, pack according to scheme (1).

e) When optically active compounds have been isolated in both racemic and enantiomeric crystal modifications, Kuroda and Mason [7] have observed that, in many cases, the density of the racemic modification is greater. Frequently, packing in a racemic modification has been described [8a,b,c] in terms of layers, or 'islands', of pure enantiomers,

TABLE I. Crystallographically Important Data Collection and Data Processing for Compound (I) and (II).

	Crystal (I)	Crystal (II)
Empirical Formula	$MoSNO_2C_{18}H_{19}$	$MoSNO_2C_{26}H_{21}$
Molecular Weight	409.36 g mol^{-1}	507.46 g mol^{-1}
Cell Constants	a = 9.264(2) A α = 76.24(3)°	a = 10.028(3) A
	b = 9.350(2) A β = 77.11(3)°	b = 12.532(7) A
	c = 12.592(5) A γ = 58.83(2)°	c = 17.774(6) A
Unit Cell Volume	899.84 A^3	2236.46 A^3
Space Group	$P\bar{1}$	$P2_12_12_1$
Density (measured)	1.51 g cm^{-3}	1.48 g cm^{-3}
(calculated)	(Z = 2) 1.511 g cm^{-3}	(Z = 4) 1.507 g cm^{-3}
Absorption Coefficient (Mo-K_α)	μ = 7.60 cm^{-1}	μ = 6.21 cm^{-1}
Radiation Used for Data Collection	Mo Kα (λ = 0.71069 A)	same
Scanning Range for 2θ	4.00° $\leqslant 2\theta \leqslant$ 60.0°	4.00° $\leqslant 2\theta \leqslant$ 72.0°
Crystal Along	[010]	$[1\bar{2}0]$
Standards for Intensity Control	$[3, 4, 5; \bar{3}, \bar{4}, \bar{5}$ and 3, 3, 3]	$[\bar{2}, 1, 1$ and $\bar{2}, \bar{7}, 0]$
Measured Every	40 reflections	2 hr exposure time
Scan Width for Each Reflection	$\Delta\theta = (0.80 + 0.40 \tan\theta)°$	$\Delta\theta = (1.10 + 0.35 \tan\theta)°$
Maximum Scan Time	5 minutes	5 minutes
Prescan Acceptance Criterion for Classifying 'Observed' Reflection	2000 counts above background	Ipre > 1.9 σ(Ipre)
Scan Technique	$\theta - 2\theta$	$\theta - 2\theta$
Total Number of Reflections Collected[a]	4129	5869
Number of Contributing Reflections in the Last Cycle of Least-Squares	3415	3160
Number of Variables	284	171
Weighting Scheme	$w = 1/(\sigma^2(F_o) + 0.002\ F_o^2)$	Unit Weights
Largest Parameter Shift in the Last Cycle of Least-Squares	0.011 σ	0.094 σ
Largest Peak in Final Difference Fourier	0.54 e A^{-3}	0.33 e A^{-3}
Final R(F)[b]	0.028	0.018
Final $R_w(F)$[c]	0.035	0.019

[a] (I): Out of 4129 reflections, 3432 having $I > 2\sigma(I)$ were classified as observed. Of these, 17 were subsequently omitted due to secondary extinction effects. (II): Out of 5868 reflections, 3165 had $I > 2\sigma(I)$; 5 were later omitted. [b] $R(F) = \Sigma(\|F_o| - |F_c\|)/\Sigma|F_o|$. [c] $R_w(F) = [\Sigma w(|F_o| - |F_c|)^2/\Sigma w|F_o|^2]^{1/2}$.

where packing within the layers is similar to that observed in the pure enantiomer, and with the 'islands' related, pairwise, through a mirror plane. The more compact crystal structures, observed for racemic mixtures, reflect their greater thermodynamic stability.

While the above considerations may be true in many cases where one compares *enantiomers*, our recent results [5] from the crystal structures of $Cp(CO)_2MoSC(CH_3)CH(i\text{-}C_3H_7)\text{-}(C_6H_5)$, in both its racemic ($P2_1/n$) and diastereomeric ($P2_1$) crystal modifications, indicate that the above considerations may not, necessarily, apply to *diastereomers*. Although the racemic modification ($P2_1/n$) does have pairs or preferred (*S*, C; *S*, Mo and *R*, C; *R*, Mo) diastereomers related to one another by mirror planes, the diastereomeric ($P2_1$) modification, with two molecules in the asymmetric unit, displays a totally different sort of packing. Despite differences in packing, the two crystal modifications have calculated densities which differ by only 0.005 g cm^{-1}, with the diastereomeric modification having the greater density. *These observations make it doubtful that density measurements would be useful in choosing between alternate packing arrangements in the case of diastereoisomeric samples.*

f) An unexpected, and somewhat startling result, discussed in our previous paper [5], is the fact that four totally independent structure determinations [of compounds with R = CH_3 but with R′ = 1) CH_3,

2) C_2H_5, 3) i-C_3H_7 (optically active, $P2_1$), and 4) i-C_3H_7, racemic, $P2_1/n$] show only small deviations in Cp-phenyl interplanar angles and in the torsional angles within the Mo–thioamide framework. When one considers the variations in packing observed in the compounds quoted above (See ref. 5 for a full discussion), it is remarkable that a conformation such as that shown in *1a* is adhered to so closely, in all cases.

All structural and spectroscopic evidence collected thus far, consistently supports the previous statements with regard to conformational and configurational preferences of preferred (*P*) Mo–thioamide complexes. At this juncture, one important question to ask in the following: 'For a given handedness of optically pure amine precursor, what is the overall conformation of the *non-preferred (NP)* diastereomer?' Such a question, when answered, could provide crucial data for an understanding of the exact mode of optical induction in these compounds.

In this report, we present the crystal and molecular structures of two additional compounds in the Mo–thioamide series: I, the racemic $Cp(CO)_2MoSC(CH_3)NCH(C_2H_5)(C_6H_5)$; and II, the optically pure $(+)_{589}$-$Cp(CO)_2MoSC(\alpha\text{-}C_{10}H_7)N\text{-}(S)\text{–}CH(CH_3)(C_6H_5)$. With the inclusion of these two compounds, new insights can be gained into the conformational preferences of this class of organometallic compounds.

Experimental

Details of the synthesis, physical properties, and spectral data of I: $(\eta^5\text{-}C_5H_5)(CO)_2MoSC(CH_3)N\text{-}CH(C_2H_5)(C_6H_5)$ and II; $(+)_{579}$-$(\eta^5\text{-}C_5H_5)(CO)_2\text{-}MoSC(\alpha\text{-}C_{10}H_7)N\text{–}CH(CH_3)(C_6H_5)$ have been reported previously [9, 10]. Both samples of crystals, provided by Brunner, are air stable and almost transparent.

During the course of this investigation, several computer software changes were made in our laboratory, both in data collection routines and in some data processing routines. In the latter stages of refinement, however, identical techniques were applied to both data sets.

A list of data collection and refinement parameters for both compounds appears in Table I.

Data Collection

For compound (I)

An orange parallelepiped (0.16 × 0.25 × 0.34 mm) was mounted, approximately along its [0 1 0] direction, onto a computer controlled CAD-4 diffractometer [11] and intensity data were collected (Mo-Kα) as described previously [1], with the following minor modifications: a) Precise cell constants were determined via a least-squares fit of 32 high angle reflections, using the PARAM routine of the X-ray '72 System of computer programs [12]. b) A comparison of the Niggli matrix (from the CAD-4 routine DETCELL), with tables provided by Roof [13], verified that the lattice was primitive and triclinic. The space group $P\bar{1}$ was chosen on the basis of cell volume, and from our knowledge that a racemic amine had been used during synthesis. The favorable refinement parameters listed in Table I verify that our choice was correct. c) Data, in the range of $4.0° \leqslant 2\theta \leqslant 60.0°$, were collected in the θ–2θ mode, using the routine SCAN in the ZIGZAG mode. During prescan (at 4 deg min^{-1}) all reflections with less than 50 counts were classified as unobserved; during a final scan, those with less than 2000 counts were also classified as unobserved, and were not used in the solution and refinement. d) The intensity standards (3, 4, 5; $\bar{3}\ \bar{4}\ \bar{5}$ and 3, 3, 3; measured every 30 reflections) showed no appreciable deviations in intensities throughout data collection.

Of a total of 4129 reflections, 3422, having $I > 2\sigma(I)$, were used in the solution and refinement stages. Of these, 17 low angle reflections were later found to exhibit large deviations in F_{obs} *vs.* $F_{calc.}$, probably from secondary extinction effects. The 17 reflections, removed from the latter refinement stages, are: 0, 1, 0; 2, 7, 2; 2, 7, 7; $\bar{2}$, $\bar{6}$, 4; 2, 6, 2; 2, 5, 3; $\bar{2}$, $\bar{5}$, 1; $\bar{2}$, $\bar{5}$, 2; $\bar{2}$, $\bar{4}$, 4; $\bar{2}$, $\bar{4}$, 2; $\bar{2}$, $\bar{4}$, 1; 2, 4, 3; 2, 3, 6; 2, 3, 1; 2, 1, 4; 2, 1, 3; and 2, 1, 2. Data reduction (with Lorentz and polarization [14] corrections) was carried out using a locally written program [15]. Due to the low absorption coefficient, absorption corrections were deemed unnecessary.

For compound II

A ruby colored prism (0.22 × 0.25 × 0.65 mm) was mounted approximately along its [1 $\bar{2}$ 0] direction, onto a CAD-4 diffractometer, employing the newer OS/4 computer software package. All diffractometer routines mentioned below may be found in the Enraf-Nonius [16] manual. Intensity data (Mo-Kα) were collected according to a more recent procedure published elsewhere [17], with the following modifications: a) A total of 25 high angle reflections, taken from each of the parity groups, were inserted into the diffractometer reference list and centered by the routine DETCELL. Precise cell constants were derived from a least-squares fit of these reflections by the routine LS. b) The Niggli matrix, calculated by the routine INDEX was compared to Roof's tables [13] to determine the crystal system and lattice symbol. The space group was determined from systematic absences. c) Data were collected in the range of $4.0° \leqslant 2\theta \leqslant 72.0°$, using the θ–2θ scan technique. During prescan (at 3.3 deg min^{-1}) the prescan intensity (Ipre) and sigma σ(Ipre)

TABLE II. Determination of the Absolute Configuration of Compound (II).

Reflection Number	Indices	F(calc.) (hkl)	F(calc.) $(\bar{h}\,\bar{k}\,\bar{l})$	Calc. F[a] ratio	Meas. F[b] ratio
1	1,4,2	33.21	34.00	0.98	0.98
2	5,4,3	39.93	41.51	0.96	0.95
3	2,1,1	96.85	98.74	0.98	0.97
4	3,3,1	73.50	75.57	0.97	0.97
5	3,1,1,	38.81	40.09	0.97	0.96
6	2,1,4	100.88	97.60	1.03	1.03
7	2,2,2	108.56	106.93	1.02	1.01
8	1,4,6	87.40	88.56	0.99	0.98
9	2,1,2	77.83	78.95	0.99	0.98
10	1,4,5	30.91	31.82	0.97	0.95

[a] Calc. F(hkl)/Calc. $F(\bar{h}\,\bar{k}\,\bar{l})$. [b] Ratio of experimentally measured $F(hkl)/F(\bar{h}\,\bar{k}\,\bar{l})$ with each reflection measured four times and averaged.

were measured. Reflections having Ipre $\geqslant 1.9\ \sigma$(Ipre) were classified as observed and measured again (with a maximum scan time of 5 minutes); those with σ(Ipre) < 0.02 were classified as unobserved. d) The $[1\ \bar{2}\ 0]$ reflection was measured at intervals of 2 hours in X-ray exposure time and showed no unusual deviations in intensity.

A total of 5868 independent reflections were collected and of these 3165, having $I \geqslant 2\sigma(I)$, were used in the solution and refinement. Five low angle reflections [1, 1, 0; 2, 2, 0; 0, 0, 2; 0, 3, 2; and 0, 2, 0] were subsequently omitted from the refinement. Lorentz and polarization [14] corrections were applied during data reduction [18]; absorption corrections were not applied.

Solution and Refinement

After data reduction, all solution and refinement routines were taken from the SHELX-76 [19] system of computer programs, using neutral atom scattering factors [20]. In both structures, Mo positions were located by the Patterson method and the remaining atoms were located in subsequent difference Fourier maps.

Compound

All hydrogens were located in difference maps and were refined with individual thermal parameters. A blocked least-squares refinement of the entire structure (3432 reflections, 284 parameters, unit weights) yielded the agreement factors:

$$R = \Sigma|(|F_o| - |F_c|)|/\Sigma|F_o| = 0.0298$$

$$R_w = [\Sigma w(|F_o| - |F_c|)^2/\Sigma w|F_o|^2]^{1/2} = 0.0349$$

After trying alternate weight routines, a final full-matrix least-squares refinement yielded the agreement parameters: R = 0.0271; R_w = 0.0350; and w = $[\sigma^2(F_o) + g\cdot F_o^2]^{1/2}$ with g = 0.002. The instrumental instability term (g) was *refined* during least-squares to an unusually small value; nonetheless, it was retained in the final calculations.

In the final refinement cycles, the instability term (g) and the overall scale factor were held constant while parameters for the 23 anisotropic non-hydrogens and 19 isotropic hydrogens were allowed to refine to the above agreement parameters, with a goodness of fit of 1.11. In the last cycle, parameters shifts were all less than 0.01 of their respective estimated standard deviations. The largest residual peak in the final difference Fourier map had a height of 0.54 electron$\cdot$Å^{-3}. Table IIIA lists the final atomic parameters.

Compound II

Although the majority of the hydrogen atoms were found in difference Fourier maps, a complete set of theoretical hydrogen positions were calculated (aliphatic d(C–H) = 1.05, aromatic d(C–H) = 0.95 Å). Positional and thermal parameters for H(19) and H(20 A, B, C) were refined (with a single group thermal parameter applied to the three methyl hydrogens) along with the non-hydrogen parameters. The cyclopentadienyl, naphthyl and phenyl hydrogens were assigned three group thermal parameters which were allowed to refine, while positional parameters were recalculated (SHELX 'floating mode') before each refinement cycle, with d(C–H) = 0.95 Å.

The final blocked least-squares refinement cycles used 3160 reflections and a total of 294 parameters; the overall scale factor and four group thermal parameters were refined in every cycle, while parameters for 31 non-hydrogens and 4 hydrogens were divided equally between the two blocks. Final agreement

TABLE IIIA. Coordinates and Thermal Parameters (×10^3, Mo & S × 10^4, H × 10^2) for Compound (I).

Atom	X/A	Y/B	Z/C	U11	U22	U33	U12	U13	U23
Mo	0.05759(2)	0.05888(2)	0.21404(1)	308(1)	331(1)	379(1)	−149(1)	−41(1)	−70(1)
S	0.26893(8)	−0.10802(8)	0.06665(5)	465(3)	492(3)	397(3)	−239(3)	−15(2)	−151(2)
O1	−0.1001(3)	−0.1583(3)	0.1971(3)	77(2)	75(2)	115(2)	−53(1)	−28(1)	−9(1)
O2	0.0345(3)	−0.1512(3)	0.4431(2)	90(2)	67(1)	45(1)	−46(1)	5(1)	−4(1)
N	0.3301(2)	−0.0417(2)	0.2277(2)	32(1)	28(1)	42(1)	−13(1)	−7(1)	−5(1)
C1	−0.1681(3)	0.2855(3)	0.1276(3)	42(1)	43(1)	65(2)	−13(1)	−22(1)	−8(1)
C2	−0.0314(3)	0.3197(3)	0.0877(3)	48(1)	39(1)	57(2)	−13(1)	−13(1)	4(1)
C3	0.0175(3)	0.3422(3)	0.1779(3)	44(1)	35(1)	79(2)	−16(1)	−21(1)	−1(1)
C4	−0.0871(3)	0.3208(3)	0.2740(3)	49(1)	41(1)	66(2)	−14(1)	−16(1)	−18(1)
C5	−0.2043(3)	0.2882(4)	0.2424(3)	33(1)	50(1)	64(2)	−12(1)	−3(1)	−17(1)
C6	0.4100(3)	−0.1240(3)	0.1449(2)	37(1)	31(1)	45(1)	−16(1)	−3(1)	−6(1)
C7	0.5989(3)	−0.2252(4)	0.1124(3)	38(1)	50(1)	72(2)	−13(1)	2(1)	−21(1)
C8	−0.0403(3)	−0.0790(3)	0.2020(3)	46(1)	48(1)	59(2)	−25(1)	−11(1)	−5(1)
C9	0.0492(3)	−0.0715(3)	0.3597(2)	48(1)	45(1)	45(1)	−24(1)	1(1)	−11(1)
C10	0.4230(3)	−0.0290(3)	0.3050(2)	37(1)	33(1)	50(1)	−14(1)	−15(1)	−6(1)
C11	0.3956(5)	−0.1126(4)	0.4212(3)	77(2)	43(1)	52(1)	−30(1)	−30(1)	4(1)
C12	0.3757(3)	0.1549(3)	0.2965(2)	35(1)	34(1)	48(1)	−16(1)	−12(1)	−7(1)
C13	0.4379(3)	0.2288(3)	0.2016(3)	40(1)	48(1)	60(2)	−23(1)	−4(1)	−7(1)
C14	0.3934(4)	0.3979(4)	0.1873(3)	50(1)	50(1)	84(2)	−32(1)	−15(1)	7(1)
C15	0.2878(4)	0.4961(4)	0.2681(3)	60(2)	38(1)	97(2)	−24(1)	−26(2)	−5(1)
C16	0.2277(4)	0.4250(4)	0.3630(3)	67(2)	46(1)	76(2)	−19(1)	−14(2)	−22(1)
C17	0.2707(4)	0.2554(3)	0.3770(3)	58(1)	44(1)	49(1)	−24(1)	−7(1)	−10(1)
C18	0.4669(7)	−0.3019(4)	0.4298(4)	120(4)	44(2)	79(2)	−38(2)	−46(3)	11(2)
H1	−0.211(4)	0.260(4)	0.074(3)	5(1)					
H2	0.015(4)	0.329(4)	0.012(3)	6(1)					
H3	0.092(4)	0.376(5)	0.177(3)	6(1)					
H4	−0.093(4)	0.330(5)	0.350(3)	7(1)					
H5	−0.308(5)	0.279(5)	0.301(4)	8(1)					
H7A	0.662(7)	−0.304(8)	0.171(5)	12(2)					
H7B	0.620(5)	−0.278(5)	0.048(4)	8(1)					
H7C	0.664(6)	−0.150(6)	0.087(4)	10(1)					
H10	0.544(4)	−0.096(4)	0.282(3)	5(1)					
H11A	0.462(3)	−0.092(4)	0.467(2)	4(1)					
H11B	0.274(5)	−0.057(5)	0.443(3)	7(1)					
H13	0.512(4)	0.164(4)	0.140(3)	6(1)					
H14	0.432(5)	0.453(6)	0.120(4)	9(1)					
H15	0.251(6)	0.616(7)	0.252(4)	11(2)					
H16	0.156(5)	0.492(6)	0.429(4)	8(1)					
H17	0.228(4)	0.221(5)	0.433(3)	6(1)					
H18A	0.466(10)	−0.346(11)	0.512(7)	20(3)					
H18B	0.424(5)	−0.322(5)	0.377(4)	8(1)					
H18C	0.587(6)	−0.349(6)	0.395(4)	9(1)					

TABLE IIIB. Coordinates and Thermal Parameters (×10^3, Mo & S × 10^4, H × 10^3).

Atom	X/A	Y/B	Z/C	U11	U22	U33	U12	U13	U23
Mo	−0.44808(2)	−0.03061(2)	−0.32025(1)	331(1)	301(1)	325(1)	−5(1)	4(1)	−12(1)
S	−0.33529(8)	−0.16775(6)	−0.23905(4)	592(4)	409(3)	355(3)	108(3)	123(3)	85(3)
O1	−0.4091(2)	0.0975(2)	−0.1725(1)	52(1)	60(1)	49(1)	−1(1)	−4(1)	−16(1)
O2	−0.3298(3)	0.1878(2)	−0.3691(1)	73(2)	40(1)	79(2)	−6(1)	8(1)	13(1)
N	−0.2756(2)	−0.1144(2)	−0.3704(1)	41(1)	36(1)	30(1)	4(1)	4(1)	0(1)
C1	−0.6555(3)	0.0329(3)	−0.3412(3)	48(2)	57(2)	157(5)	5(2)	−38(2)	7(3)
C2	−0.6695(3)	−0.0496(4)	−0.2914(2)	31(1)	115(3)	77(2)	−15(2)	8(2)	−22(2)
C3	−0.6367(3)	−0.1429(3)	−0.3284(3)	43(2)	52(2)	156(4)	−16(2)	−8(3)	−9(3)
C4	−0.6029(4)	−0.1180(6)	−0.3998(3)	50(2)	178(6)	113(4)	−42(3)	17(2)	−102(4)

(continued on facing page)

TABLE IIIB. *(continued)*

Atom	X/A	Y/B	Z/C	U11	U22	U33	U12	U13	U23
C5	−0.6126(5)	−0.0104(6)	−0.4083(3)	74(3)	196(7)	67(3)	−57(4)	−39(2)	37(4)
C6	−0.4212(2)	0.0497(2)	−0.2276(1)	32(1)	37(1)	44(1)	0(1)	0(1)	0(1)
C7	−0.3664(3)	0.1039(2)	−0.3536(2)	43(1)	41(1)	42(1)	2(1)	2(1)	3(1)
C8	−0.2404(2)	−0.1813(2)	−0.3192(2)	40(1)	31(1)	34(1)	2(1)	−1(1)	−3(1)
C9	−0.1322(2)	−0.2633(2)	−0.3209(2)	37(1)	36(1)	35(1)	3(1)	0(1)	0(1)
C10	−0.0130(3)	−0.2434(3)	−0.2865(2)	46(2)	47(2)	48(2)	−2(1)	−8(1)	−2(1)
C11	0.0840(3)	−0.3233(3)	−0.2807(2)	36(2)	68(2)	58(2)	3(1)	−8(1)	9(2)
C12	0.0620(3)	−0.4226(2)	−0.3096(2)	43(1)	57(2)	56(2)	15(1)	5(2)	15(1)
C13	−0.0581(3)	−0.4463(2)	−0.3466(1)	44(1)	38(1)	40(1)	7(1)	12(1)	8(1)
C14	−0.0852(3)	−0.5485(2)	−0.3769(2)	67(2)	37(1)	52(2)	11(1)	18(1)	5(1)
C15	−0.2038(4)	−0.5697(2)	−0.4106(2)	79(2)	35(1)	59(2)	−8(2)	16(2)	−7(1)
C16	−0.3019(3)	−0.4918(2)	−0.4156(2)	59(2)	47(2)	55(2)	−14(1)	4(2)	−6(1)
C17	−0.2814(3)	−0.3918(2)	−0.3876(2)	41(1)	41(1)	49(2)	−3(1)	3(1)	−3(1)
C18	−0.1584(3)	−0.3660(2)	−0.3524(1)	36(1)	32(1)	35(1)	3(1)	5(1)	2(1)
C19	−0.2065(3)	−0.1108(2)	−0.4444(1)	52(2)	44(1)	32(1)	10(1)	10(1)	2(1)
C20	−0.3023(4)	−0.1430(3)	−0.5067(2)	83(3)	69(2)	34(1)	−12(2)	7(2)	−5(2)
C21	−0.1411(3)	−0.0027(2)	−0.4557(1)	43(1)	47(1)	35(1)	8(1)	12(1)	4(1)
C22	−0.0456(3)	0.0323(3)	−0.4046(2)	54(2)	59(2)	51(1)	4(2)	0(2)	6(2)
C23	0.0188(3)	0.1283(3)	−0.4135(2)	54(2)	67(2)	72(2)	−4(2)	8(2)	−9(2)
C24	−0.0089(4)	0.1916(3)	−0.4749(2)	75(2)	49(2)	73(2)	0(2)	31(2)	−4(2)
C25	−0.1022(4)	0.1590(3)	−0.5257(2)	99(3)	50(2)	51(2)	6(2)	15(2)	10(2)
C26	−0.1688(4)	0.0629(2)	−0.5165(2)	70(2)	53(2)	40(1)	7(2)	3(2)	5(1)
H1	−0.6724(3)	0.1062(3)	−0.3316(3)	117(7)					
H2	−0.6969(3)	−0.0434(4)	−0.2404(2)	117(7)					
H3	−0.6377(3)	−0.2125(3)	−0.3072(3)	117(7)					
H4	−0.5770(4)	−0.1672(6)	−0.4377(3)	117(7)					
H5	−0.5929(5)	0.0284(6)	−0.4529(3)	117(7)					
H10	0.0042(3)	−0.1746(3)	−0.2661(2)	57(4)					
H11	0.1663(3)	−0.3082(3)	−0.2565(2)	57(4)					
H12	0.1283(3)	−0.4762(2)	−0.3045(2)	57(4)					
H14	−0.0195(3)	−0.6029(2)	−0.3737(2)	57(4)					
H15	−0.2201(4)	−0.6387(2)	−0.4307(2)	57(4)					
H16	−0.3845(3)	−0.5082(2)	−0.4390(2)	57(4)					
H17	−0.3494(3)	−0.3394(2)	−0.3916(2)	57(4)					
H19	−0.1430(30)	−0.1616(23)	−0.4417(15)	55(9)					
H20A	−0.3718(33)	−0.0886(26)	−0.5098(18)	59(6)					
H20B	−0.3415(34)	−0.2106(24)	−0.4988(19)	59(6)					
H20C	−0.2650(33)	−0.1432(27)	−0.5492(18)	59(6)					
H22	−0.0243(3)	−0.0113(3)	−0.3626(2)	81(5)					
H23	0.0825(3)	0.1510(3)	−0.3773(2)	81(5)					
H24	0.0364(4)	0.2574(3)	−0.4817(2)	81(5)					
H25	−0.1217(4)	0.2027(3)	−0.5680(2)	81(5)					
H26	−0.2342(4)	0.0418(2)	−0.5522(2)	81(5)					

factors of $R = 0.0184$ and $R_w = 0.0199$ were obtained, using unit weights. During the last cycle, the magnitude of parameter shifts were all less than 0.10 of their respective esd's. The largest peak in the final difference map appeared close to Mo, with a height of 0.33 e·$Å^{-3}$. Final atomic parameters appear in Table IIIB.

Absolute configuration of compound II

After the original refinement was finished, a separate refinement was performed on structure II, using a set of inverted (x, y, z → −x, −y, −z) coordinates (The UNDO-1 function of the SHELX system inverts coordinates and allows for proper handling of anisotropic thermal parameters). After several cycles of blocked least-squares refinement, the inverted structure converged to the agreement parameters: $R = 0.0213$ and $R_w = 0.0229$. Comparison of agreement parameters from the two parallel refinements, by the Hamilton [21] R-ratio test, indicated a significant difference between the two refinements at the 99.5% confidence level. Comparison of calculated structure factors from the two refinements yielded many reflections suitable for direct determination of the

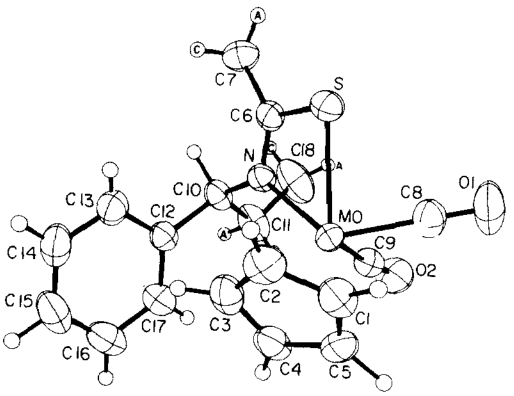

Fig. 1. ORTEP plot of Compound I showing numbering scheme. Non-hydrogen atoms are represented by 50% probability ellipsoids. Hydrogen atoms are represented by spheres of convenient size.

absolute configuration, via the Bijvoet method [22]. As shown in Table II, ten such reflections were selected and, for each one, both (hkl) and $(\overline{hkl})$ were measured four times. The reflections were inserted (24 at a time) into the diffractometer reference list, and were measured as intensity standards, using the normal data collection routine, DATCOL. Intensity data were reduced to structure factor amplitudes which were averaged and compared, as shown in Table II. Comparison of the F ratios, consistently, shows the original configuration (the one refined throughout and presented in Table IIIB) to be the correct one. In this non-preferred configuration, the optically active carbon, C(19), derived from the parent optically active amine, displays its known (*S*) configuration. Using the extension of the *R*, *S* system [23] to polyhapto ligands in organometallic complexes [24], the priority sequence of the ligands is $(\eta^5\text{-}C_5H_5) > S > N > C(CO)$. Thus, according to the sequence rule of the *R*, *S* system and the line of sight convention [4], the configuration at the Mo atom is (*R*). The correct absolute configuration of (II) can be seen in the ORTEP [25] diagrams, Figs. 3, 4 and 8.

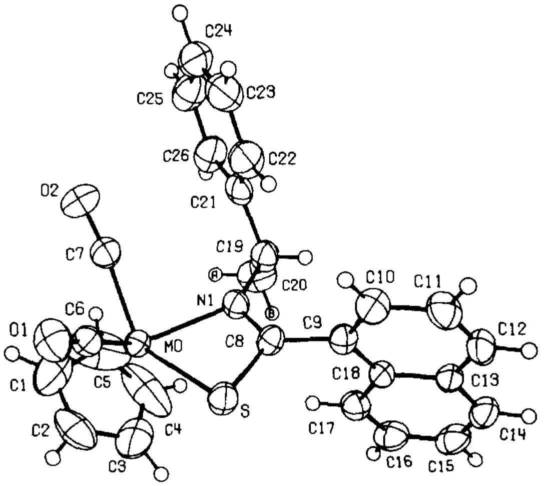

Fig. 3. ORTEP plot of Compound II showing numbering scheme. Non-hydrogen atoms are represented by 50% probability ellipsoids. Hydrogen atoms are represented by spheres of convenient size.

Results and Discussion

Molecular Geometry

Similarities in the Cp(CO)$_2$MoSCN fragments

As shown in Figs. 1–4, structures (I) and (II) both contain a central Mo atom surrounded by a set of five ligands distributed in a square pyramidal arrangement, with $(\eta^5\text{-}C_5H_5)$ in the axial position. The thioamide is bound to Mo through both its S and N atoms [26]. Similarities in the $Cp(CO)_2$-MoSCN fragments of (I) and (II) can be seen in the tables of bonding parameters (Tables III–VI) as well as in Figs. 3–5. Table VII shows a comparison of selected parameters for the $Cp(CO)_2MoSCN$ fragment in the six Mo-thioamide complexes already described. So far as the central fragment is concerned (see Table VII) all compounds in this series possess the same basic geometry (neglecting chirality for the moment). In a previous paper [1], we describ-

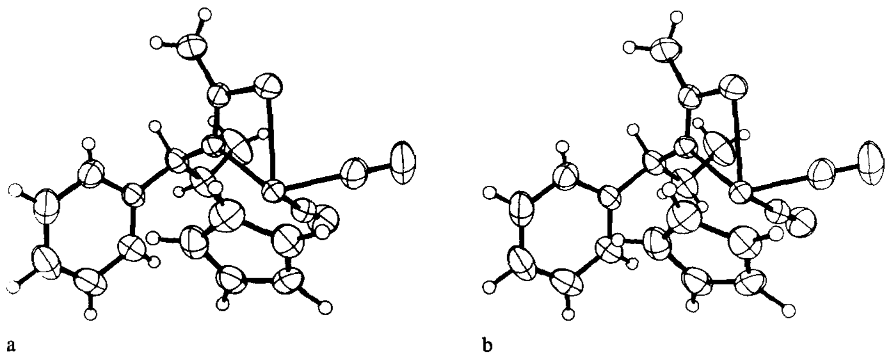
a

b

Fig. 2. Stereo view of Compound I.

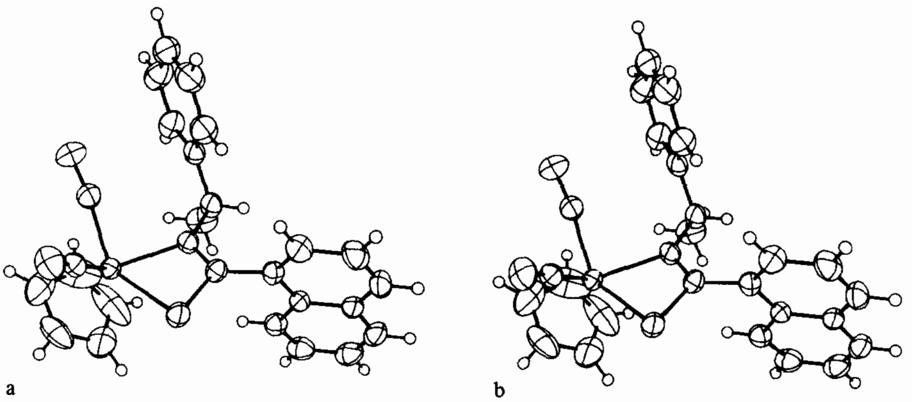

Fig. 4. Stereo view of Compound II.

Fig. 5. BMFIT stereo view showing similarities between Compounds I and II in the orientation of cyclopentadienyl rings.

TABLE IV. Bond Lengths (Å) and Angles (°) for Compounds (I) and (II).

a) Bond Lengths Common to Both Compounds.	Compound (I)		Compound (II)
Mo–S	2.511(1)	Mo–S	2.513(1)
Mo–N	2.224(2)	Mo–N	2.211(2)
Mo–C(1)	2.319(2)	Mo–C(1)	2.258(4)
Mo–C(2)	2.411(3)	Mo–C(2)	2.292(3)
Mo–C(3)	2.417(3)	Mo–C(3)	2.362(4)
Mo–C(4)	2.323(3)	Mo–C(4)	2.368(5)
Mo–C(5)	2.281(3)	Mo–C(5)	2.288(5)
Mo–C(8)	1.967(3)	Mo–C(6)	1.949(3)
Mo–C(9)	1.956(3)	Mo–C(7)	1.965(3)
S–C(6)	1.733(2)	S–C(8)	1.722(3)
N–C(6)	1.294(3)	N–C(8)	1.287(3)
C(6)–C(7)	1.509(3)	C(8)–C(9)	1.494(3)
N–C(1)	1.296(3)	N–C(19)	1.488(3)
C(1)–C(2)	1.420(4)	C(1)–C(2)	1.369(7)
C(2)–C(3)	1.408(4)	C(2)–C(3)	1.382(6)
C(3)–C(4)	1.416(5)	C(3)–C(4)	1.350(8)
C(4)–C(5)	1.422(4)	C(4)–C(5)	1.361(10)
C(5)–C(1)	1.412(4)	C(5)–C(1)	1.379(7)
C(10)–C(11)	1.521(4)	C(19)–C(20)	1.521(5)
C(12)–C(13)	1.396(4)	C(21)–C(22)	1.391(4)
C(13)–C(14)	1.387(4)	C(22)–C(23)	1.375(5)
C(14)–C(15)	1.380(5)	C(23)–C(24)	1.377(5)
C(15)–C(16)	1.374(5)	C(24)–C(25)	1.363(5)

(continued overleaf)

TABLE IV. *(continued)*

a) Bond Lengths Common to Both Compounds.	Compound (I)		Compound (II)
C(16)–C(17)	1.396(4)	C(25)–C(26)	1.387(5)
C(17)–C(12)	1.387(4)	C(26)–C(21)	1.387(4)
C(8)–O(1)	1.150(3)	C(6)–O(1)	1.154(3)
C(9)–O(2)	1.161(3)	C(7)–O(2)	1.147(4)
b) Additional Bond Lengths for Compound (I).			
C(11)–C(18)	1.521(4)	C(11)–H(11A)	1.04(3)
C(1)–H(1)	0.99(3)	C(11)–H(11B)	0.97(4)
C(2)–H(2)	0.96(3)	C(13)–H(13)	1.00(4)
C(3)–H(3)	0.90(3)	C(14)–H(14)	0.98(4)
C(4)–H(4)	0.98(4)	C(15)–H(15)	0.97(6)
C(5)–H(5)	1.10(4)	C(16)–H(16)	1.04(4)
C(7)–H(7A)	0.96(6)	C(17)–H(17)	0.81(4)
C(7)–H(7B)	0.98(4)	C(18)–H(18A)	1.02(9)
C(10)–H(10)	0.97(3)	C(18)–H(18C)	1.00(5)
c) Additional Bond Lengths for Compound (II).			
C(9)–C(10)	1.366(4)	C(17)–C(18)	1.420(4)
C(10)–C(11)	1.400(4)	C(18)–C(9)	1.427(3)
C(11)–C(12)	1.364(4)	C(13)–C(18)	1.427(4)
C(12)–C(13)	1.404(4)	C(19)–H(19)	0.90(3)
C(13)–C(14)	1.416(4)	C(20)–H(20A)	0.98(3)
C(14)–C(15)	1.357(5)	C(20)–H(20B)	0.94(3)
C(15)–C(16)	1.389(5)	C(20)–H(20C)	0.84(3)
C(16)–C(17)	1.363(4)	All other C–H	0.95
Compound (I)		Compound (II)	
d) Bond Angles Common to Both Compounds.			
S–Mo–N	63.6(1)	S–Mo–N	63.6(1)
S–Mo–C(8)	79.8(1)	S–Mo–C(6)	78.8(1)
S–Mo–C(9)	115.8(1)	S–Mo–C(7)	124.9(1)
N–Mo–C(8)	124.6(1)	N–Mo–C(6)	118.6(1)
N–Mo–C(9)	86.3(1)	N–Mo–C(7)	87.7(1)
C(8)–Mo–C(9)	73.4(1)	C(6)–Mo–C(7)	75.8(1)
Mo–S–C(6)	81.4(1)	Mo–S–C(8)	80.9(1)
S–C(6)–C(7)	120.0(2)	S–C(8)–C(9)	119.1(2)
S–C(6)–N	111.1(2)	S–C(8)–N	111.6(2)
N–C(6)–C(7)	128.9(2)	N–C(8)–C(9)	129.2(2)
Mo–N–C(10)	134.5(1)	Mo–N–C(19)	135.0(3)
Mo–N–C(6)	103.8(1)	Mo–N–C(8)	103.8(2)
N–C(10)–C(11)	111.5(2)	N–C(19)–C(20)	110.0(3)
N–C(10)–C(12)	109.0(2)	N–C(19)–C(21)	110.2(2)
C(12)–C(13)–C(14)	121.2(3)	C(21)–C(22)–C(23)	121.7(3)
C(13)–C(14)–C(15)	120.2(3)	C(22)–C(23)–C(24)	120.0(3)
C(14)–C(15)–C(16)	119.5(3)	C(23)–C(24)–C(25)	119.5(3)
C(15)–C(16)–C(17)	120.3(3)	C(24)–C(25)–C(26)	120.8(3)
C(16)–C(17)–C(12)	121.0(3)	C(25)–C(26)–C(21)	120.7(3)
C(17)–C(12)–C(13)	117.7(2)	C(26)–C(21)–C(22)	117.4(3)
C(1)–C(2)–C(3)	107.9(3)	C(1)–C(2)–C(3)	107.8(4)
C(2)–C(3)–C(4)	108.3(2)	C(2)–C(3)–C(4)	108.2(4)
C(3)–C(4)–C(5)	107.9(3)	C(3)–C(4)–C(5)	108.4(5)
C(4)–C(5)–C(1)	107.6(2)	C(4)–C(5)–C(1)	108.4(5)
C(5)–C(1)–C(2)	108.3(2)	C(5)–C(1)–C(2)	107.2(4)
Mo–C(8)–O(1)	178.4(3)	Mo–C(6)–O(1)	178.1(2)
Mo–C(9)–O(2)	174.1(2)	Mo–C(7)–O(2)	172.6(3)

(continued on facing page)

TABLE IV. *(continued)*

e) Additional Bond Angles for Compound (I).

C(19)–C(11)–C(18)	113.2(3)	H(19)–C(10)–N	107(2)
H(11A)–C(11)–H(11B)	114(3)	H(10)–C(10)–C(11)	105(2)
		H(10)–C(10)–C(12)	110(2)

f) Additional Bond Angles for Compound (II).

C(9)–C(10)–C(11)	120.6(3)	C(17)–C(18)–C(9)	120.1(2)
C(10)–C(11)–C(12)	120.9(3)	C(18)–C(9)–C(10)	120.1(2)
C(11)–C(12)–C(13)	120.5(3)	C(12)–C(13)–C(18)	119.3(2)
C(12)–C(13)–C(14)	122.3(2)	C(14)–C(13)–C(18)	118.4(3)
C(13)–C(14)–C(15)	120.9(3)	C(9)–C(18)–C(13)	118.5(2)
C(14)–C(15)–C(16)	120.7(3)	C(17)–C(18)–C(13)	118.9(2)
C(15)–C(16)–C(17)	121.0(3)	H(19)–C(19)–N	105(2)
C(16)–C(17)–C(18)	120.1(3)	H(19)–C(19)–C(20)	107(2)
		H(19)–C(19)–C(21)	109(2)

TABLE V. Least Squares Planes (in Orthogonal Å Space) and Deviations of Atoms from these Planes (in Å).

Compound (I)

(a) Plane Based on C(1), C(2), C(3), C(4) and C(5)

$$-0.1994x \quad +0.9684y \quad -0.1499z \quad = \quad 2.170$$

C(1)	−0.0048	C(2)	−0.0000	C(3)	0.0048
C(4)	−0.0077	C(5)	0.0077	Mo	−2.0133

(b) Plane Based on C(12), C(13), C(14), C(15), C(16) and C(17).

$$-0.8823x \quad +0.1941y \quad -0.4287z \quad = \quad -5.673$$

C(12)	0.0060	C(13)	−0.0073	C(14)	0.0016
C(15)	0.0053	C(16)	−0.0065	C(17)	0.0008
H(10)	0.0563	H(3)	2.5962		

(c) Plane Based on S, N, C(8) and C(9).

$$-0.0713x \quad +0.9666y \quad -0.2461z \quad = \quad -0.964$$

S	−0.1076	N	0.1089	C(8)	0.1153
C(9)	−0.1166	Mo	1.0517		

(d) Plane Based on Mo, S, N and C(6)

$$0.3391x \quad +0.7629y \quad -0.5504z \quad = \quad -0.290$$

Mo	−0.0057	S	0.0077	N	0.0118
C(6)	−0.0137	C(7)	−0.0626		

(e) Plane Based on N, C(10), C(11) and C(12)

$$0.7689x \quad -0.5548y \quad -0.3177z \quad = \quad 1.877$$

N	−0.1096	C(10)	0.3347	C(11)	−0.1139
C(12)	−0.1112				

(continued overleaf)

TABLE V. *(continued)*

(f) Equations of Lines in Orthogonal Å Space.
(α) Line defined by C(10) and C(11).

L(1) = I = (4.4696) + (−0.2185) T
L(2) = J = (0.0880) + (0.3024) T
L(3) = K = (4.4088) + (0.9278) T

(β) Line defined by C(10) and C(12).

L(1) = I = (4.8495) + (0.2811) T
L(2) = J = (1.0458) + (0.9573) T
L(3) = K = (3.6519) + (0.0681) T

Compound (II)

(a) Plane Based on C(1), C(2), C(3), C(4) and C(5).

$$-0.9522x \quad -0.1081y \quad -0.2856z \quad = \quad 7.942$$

C(1)	0.0051	C(2)	−0.0025	C(3)	−0.0011
C(4)	0.0043	C(5)	−0.0058	Mo	−1.9961

(b) Plane Based on C(21), C(22), C(23), C(24), C(25) and C(26).

$$0.7134x \quad -0.4612y \quad -0.5276z \quad = \quad 3.278$$

C(21)	0.0019	C(22)	0.0042	C(23)	−0.0073
C(24)	0.0042	C(25)	0.0019	C(26)	−0.0049

(c) Plane Based on C(21), C(22), C(23), C(24), C(25) and C(26).

$$-0.9128x \quad -0.2679y \quad -0.3081z \quad = \quad 4.939$$

S	0.0031	N	−0.0031	C(6)	−0.0033
C(7)	0.0032	Mo	1.0198		

(d) Plane Based on Mo, S, N and C(8).

$$-0.6225x \quad -0.6968y \quad -0.3564z \quad = \quad 5.084$$

Mo	0.0089	S	−0.0120	N	−0.0186
C(8)	0.0216	C(19)	0.0124		

(e) Plane Based on N, C(19), C(20) and C(21).

$$-0.7305x \quad -0.6828y \quad -0.0152z \quad = \quad 1.021$$

N	0.1189	C(19)	−0.3373	C(20)	0.1063
C(21)	0.1122				

(f) Equations of Lines in Orthogonal Å Space.
(α) Line defined by C(19) and C(20).

L(1) = I = (−2.5510) + (−0.3786) T
L(2) = J = (−1.7926) + (−0.3169) T
L(3) = K = (−8.4528) + (−0.8696) T

(β) Line defined by C(19) and C(21).

L(1) = I = (−1.7427) + (−0.4316) T

(continued on facing page)

TABLE V. *(continued)*

L(2) = J = (−0.7116) + (0.8924) T
L(3) = K = (−7.9920) + (−0.1319) T

(g) Plane Based on C(9), C(10), C(11), C(12), C(13), C(14), C(15), C(16), C(17), and C(18).

$$0.3836x \quad +0.2932y \quad -0.8757z \quad = \quad 3.516$$

C(9)	0.0038	C(10)	−0.0011	C(11)	−0.0107
C(12)	−0.0107	C(13)	0.0165	C(14)	0.0079
C(15)	−0.0018	C(16)	−0.0151	C(17)	−0.0048
C(18)	0.0160				

Angles between Planes (°).

		Angle	
Plane 1	Plane 2	Compound (I)	Compound (II)
(a)	(b)	64.65	61.40
(a)	(d)	41.09	39.66
(b)	(d)	85.13	86.26
(e)	(d)	89.25	90.89
(g)	(d)	–	97.53

Angles between Lines and Planes (°).

		Angle	
Plane 1	Plane 2	Compound (1)	Compound (II)
(α)	(d)	56.08	39.97
(β)	(d)	37.99	72.17

TABLE VI. Selected Torsional Angles.[a]

Compound (I)					Compound (II)				
Atoms				Angle[b]	Atoms				Angle
A	B	C	D		A	B	C	D	
C(8)	Mo	S	C(6)	136.16	C(6)	Mo	S	C(8)	−131.60
C(8)	Mo	N	C(6)	−52.95	C(6)	Mo	N	C(8)	60.03
C(6)	N	C(10)	C(11)	116.90	C(8)	N	C(19)	C(20)	114.92
C(6)	N	C(10)	C(12)	−115.75	C(8)	N	C(19)	C(21)	−118.08
N	C(10)	C(12)	C(13)	71.68	N	C(19)	C(21)	C(22)	59.36
N	C(10)	C(12)	C(17)	−106.91	N	C(19)	C(21)	C(26)	−122.79
N	C(10)	C(11)	C(18)	63.80	N	C(8)	C(9)	C(10)	100.46
					N	C(8)	C(9)	C(18)	−85.48

[a] According to the IUPAC-IUP convention [54], a positive (+) torsional angles in the fragment ABCD represent a clockwise rotation of bond AB about the line of sight (BC) so as to eclipse CD with AB. [b] The torsional angles listed for compound (I) correspond to the molecule depicted in Figure 2a. To obtain torsional angles for the other enantiomer, in the centrosymmetric unit cell, the reader need only invert the signs of the torsional angles listed.

ed the stereochemistry of the Cp(CO)$_2$ MoSCN fragment and compared it with other molybdenum complexes and to other bound and unbound thioamides. During the course of this investigation, we have noticed three additional features of the Cp(CO)$_2$-MoSCN fragment that were not discussed previously.

a) In our preceding paper [5] we noted that several structures in the Mo–thioamide series show significant deviations in their Mo–S and Mo–N

TABLE VIIA. A Comparison of Bond Distances in $\mathrm{CpMo(CO)_2SC(R)NCH(R')(C_6H_5)}$ Complexes.

R	R′	Mo–S	Mo–N	Mo–C=O^a	C=O^a	Mo–C(Cp) (Average)	S–C	N–C	Ref.
CH_3	CH_3	2.514(1)	2.209(3)	1.949(5) 1.966(5)	1.151(7) 1.144(7)	2.355	1.731(3)	1.306(5)	1
CH_3	CH_2CH_3	2.511(1)	2.224(2)	1.956(3) 1.967(3)	1.161(3) 1.150(3)	2.350	1.733(2)	1.294(3)	This study
CH_3	i-C_3H_7	2.5113(8)	2.220(2)	1.947(3) 1.957(3)	1.167(4) 1.167(3)	2.340	1.719(3)	1.303(3)	5
CH_3	i-C_3H_7	2.5072(9)	2.231(2)	1.953(3) 1.968(3)	1.163(4) 1.154(4)	2.348	1.718(3)	1.304(3)	5
CH_3	i-C_3H_7	2.501(2)	2.225(6)	1.951(8) 1.966(8)	1.16(1) 1.16(1)	2.330	1.760(7)	1.281(10)	5
α-$C_{10}H_7$	CH_3	2.513(1)	2.211(2)	1.949(3) 1.965(3)	1.154(3) 1.147(4)	2.314	1.722(3)	1.287(3)	This study
Average Values		2.510(5)	2.220(9)	1.951(3) 1.965(4)	1.159(6) 1.154(9)	2.34(2)	1.73(2)	1.30(1)	

^{a}Values *trans* to S and N, respectively.

TABLE VIIB. A Comparison of Bond Angles in $\mathrm{CpMo(CO)_2SC(R)NCH(R')(C_6H_5)}$ Complexes.

R	R′	S–Mo–N	S–Mo–CO (*cis*)	S–Mo–CO (*trans*)	N–Mo–CO (*cis*)	N–Mo–CO (*trans*)	CO–Mo–CO	Ref.
CH_3	CH_3	63.79(8)	78.5(2)	112.8(2)	88.5(2)	118.4(2)	72.82	1
CH_3	CH_2CH_3	63.6(1)	79.8(1)	115.8(1)	86.3(1)	124.6(1)	73.4(1)	This study
CH_3	i-C_3H_7	63.84(6)	81.63(9)	126.1(1)	88.9(1)	119.7(1)	72.8(1)	5
CH_3	i-C_3H_7	63.77(6)	80.74(9)	125.6(1)	86.7(1)	118.3(1)	74.6(1)	5
CH_3	i-C_3H_7	63.7(2)	79.8(3)	123.6(3)	87.1(3)	118.8(3)	73.9(3)	5
α-$C_{10}H_7$	CH_3	63.6(1)	87.8(1)	124.9(1)	87.7(1)	118.6(1)	73.4(1)	This study

distances (from their group mean values of 2.510(5) and 2.220(9) Å). For most compounds in the series, the two bond deviations are inversely related (*i.e.* an increase in Mo–S is accompanied by a decrease in Mo–N). With the inclusion of compounds (I) and (II) on Table VII, there still appears to be *no simple correlation* between these bond deviations and such factors as: 1) *trans*-S–Mo–C(O) and N–Mo–C(O) angles; 2) bulkinesss of R′ substituents; 3) basicity of amine precursors; or 4) overall conformation of the compound (preferred *vs.* non-preferred).

b) A second trend, which was not discussed in any of our previous papers, pertains to the *trans*-influence of both S and N atoms upon Mo–C(O) distances in square-pyramidal complexes. On Table VIIA, one finds the average Mo–C(O) distance for carbonyls *trans* to S to be 1.965(4) Å, whereas the distance *trans* to N is 1.951(3) Å. Although the average deviation in Mo–C(O) distances is small (approx. 0.014 Å) it is consistent, appearing throughout the Mo–thioamide series.

In idealized geometries, the generally accepted interpretation of *trans*-influences has been in terms of competition, by ligands, for metal electron density; thus, whether defined in terms of σ-donor/π-acceptor properties [27a–c] or in terms of favorable metal–ligand orbital overlap [28], a *stronger* ligand will tend to draw electron density from a metal orbital, weakening (and lengthening) any other M–L bonds using the same metal orbital. A similar argument has been used to explain *cis*-influences in cases where two ligands share adjacent lobes of a metal d-orbital; *cis*-influences, however, are found to be smaller in magnitude than *trans*-influences for a given ligand [29]. From the S–Mo–C(O) and N–Mo–C(O) angles listed in Table VIIB one may describe the deviations in Mo–C(O) distances for square-pyramidal Mo–thioamides in terms of either *cis*- or *trans*-influences, however, considering the magnitude of the bond length deviations, we will discuss the deviations as the result of *trans*- rather than *cis*- directed influences.

Trans influences have been studied at great length in complexes of idealized (square planar and octahedral) geometries, and have been reviewed elsewhere [27a–c]. In several octahedral complexes involving only S and N ligands, R. C. Elder, *et al.* [30] observed a 0.04 deviation for Cr–N and Co–N

TABLE VIII. Comparison of *cis*-$Cp(CO)_2ML_1L_2$ Complexes.

Compound	Deviation in M–C(O) Distance(s) (Å)	*Trans* Angles (°)		L_2 Ligand Eclipsed By C(cp)	C–Cp–M–L2 Torsion Angle (°)	Reference
		C–M–L_1	C–M–L_2			
$CpV(CO)_4$	0	~120	~120	disordered	–	33a
$CpNb(CO)_4$	0	~120	~120	disordered	–	33b
	0.02	117.8	117.8	disordered	–	33c
$CpMo(CO)_3Cl$	0.022	106.9	136.6	Cl	–4.38	33d
$CpMo(CO)_3C_2H_5$	0.01	–	–	C_2H_5	–	33e
$CpMo(CO)_3C_3F_7$	0.012	116.9	131.9	C_3F_7	3.14	33f
$CpMo(CO)_3CH_2CO_2Et$	0.01	108.8	131.9	CH_2CO_2Et	–	33g
$[(Cp)W(CO)_3I\text{-})_3Ag]^+BF_4^-$	0.022	110.5	134.4	I	7.59	33h
$Cp(CO)_2MoP(N\text{-but})_3I$	0.241	135.0	119.1	P	0.92	33i
$Cp(CO)_2MoNH_2CH_2CH_2C{=}O$	0.048	121.7	122.8	N		33j
$Cp(CO)_2MoHNHC(CO_2Et)COH$	0.057	123.1	118.9	N	–	33k
$Cp(CO)_2MoN(Me)\text{-}C(Me)C(Ph)C{=}O$	0.012	119.0	124.2	N	4.40	33l
$Cp(CO)_2MoSC(R)NH(R')Ph$						
$R = CH_3$ $R' = CH_3$	–0.017	18.4	112.8	S	2.01	
$R = CH_3$ $R' = C_2H_5$	0.011	115.8	124.6	N	0.37	This work
$R = CH_3$ $R' = i\text{-}C_3H_7$	0.010	126.1	119.7	N	3.91	5
	0.015	125.6	118.3	N	–8.09	5
$R = CH_3$ $R' = i\text{-}C_3H_7$	0.015	123.6	118.8	N	–1.99	This work
$R = \alpha\text{-}C_{10}H_7$ $R' = CH_3$	0.016	124.9	118.6	N	–1.94	This work
$Cp(CO)_2MoP(Ph_2)NH(Me)CH(Me)(Ph)Cl$	0.059	136.3	125.9	Cl	–6.75	34a
$Cp(CO)_2MoSC(CHMePh)(\alpha\text{-}C_5H_4N)$	0.082	121.5	127.5	N		34b

distances *trans* to sulfur. In comparing the mutual influence of S, N and CO ligands in known structures, it is important that comparisons be made between equivalent bonding parameters: An examination of the octahedral $[Me_3CSC_2H_4SCMe]Cr(CO)_4$ [31] and $[Me_2NC_2H_4NMe_2]Cr(CO)_4$ [32] structures shows the average Cr–C(O) distances for carbonyls *trans* to S and N to be 1.820 and 1.834 Å. At first, this would seem to attribute a greater *trans* influence to sulfur-containing ligands. A closer look at bonding parameters for the above two complexes shows that in going from bidentate S,S to N,N ligands, all four Cr–C(O) distances decrease. In the two compounds, the average deviation in Cr–C(O) distances (axial-equatorial, for carbonyls *trans* to S and N respectively) are –0.041 and –0.065 Å. The larger internal deviation in Cr–C(O) distances for the nitrogen containing complex indicates that N exerts the stronger *trans* influence. In the octahedral $[S(CH_2)_3SC{=}C(OEt)C(OEt)NH]Cr(CO)_4$ [32] complex having both S and N ligands atoms in equatorial positions, the deviations in *trans*-Cr–C(O) distances is 0.019 Å, with the longer distance appearing *trans* to N. This deviation is smaller than the 0.024 Å difference in *trans* influences for the pair of compounds cited above, and is slightly larger than the 0.014 Å found (throughout Table VIIA) for square-pyramidal Mo-thioamide complexes. In all cases, a comparison of equivalent bonding parameters for S and N ligands show N to exert a slightly stronger *trans* influence; both ligands, however, are weaker than carbonyl.

c) A final trend concerning the central $Cp(CO)_2$-MoSCN fragments involves the orientation of apical Cp rings, relative to the basal ligands in square-pyramidal complexes. Figure 5 shows a Best Molecular FIT [35] diagram of the central fragments in (I) and (II), viewed approximately down their common Cp(centroid)–Mo vector. The two compounds possess an identical orientation of Cp rings; *i.e.,* two Cp carbons eclipsing S and N, while the remaining Cp carbons are staggered with respect to the carbonyls. For a Cp-capped square-pyramidal complex, one may calculate torsion angles about the Cp–Metal vector, involving pairs of apical and basal ligand atoms. For an ideal $CpML_4$ complex, geometry dictates that the minimum torsional angle must range in value from –9 to +9°. Table VIII shows that the minimum torsional angles in Mo-thioamides span a range of –1.94 to 8.09°. Although little can be said about the values of individual torsion angles, something can be said for the basal ligands associated with the smallest angles: Within the Mo-thioamide series, these minimum torsional angles are always associated with S or N atoms, rather than carbonyls.

In a recent study of cyclobutadienyl-capped trigonal-pyramidal complexes (η^4-$R_4C_4ML_3$), Davis and Riley [36] made a study of cyclobutadiene orientations, and found the smallest C–Cp–Mo–L torsion angles to span the entire theoretical range of –15 to 15°. Similar structural and theoretical investigations of $CpML_3$ complexes [37] predict an extremely small (0.002 kcal/mol) rotational barrier between the Cp and ML_3 fragments. Finally, more recent calculations on $CpML_4$ complexes [38a] predict a similar 'minuscule' rotational barrier, again, as the result of orbital degeneracy. In all of the above studies, it was assumed that the rotational barrier of the apical group would increase *only slightly* [38b], as orbital degeneracy is removed through ligand substitutions; as a result, it was expected that the equilibrium (solid state) orientation of an apical group would be determined, more from external (packing) forces than from any electronic effects. Although this conclusion appears to be valid for η^4-$R_4C_4ML_3$ and $CpML_3$ complexes, data presented in Table VIII for $CpML_4$ complexes, having *cis*-dicarbonyls as basal ligands, show that within this class (a total of *18* structures), there is some regularity in the orientation of apical Cp rings. Such regularity was originally suggested in the early 1970s [33e] and data added since then, particularly in our own series, lend considerable weight to the earlier speculations.

In attempting to explain the orientation of Cp rings in $CpML_4$ complexes, listed on Table VIII, one may think in terms of internal electronic effects, intra-molecular steric effects, or in terms of inter-molecular packing forces. As we have already shown (see ref. 5 and Table IX), Mo-thioamide complexes adopt a variety of packing arrangements, in both polar and non-polar space groups. Also, there are substantial differences in the intra-molecular contacts experienced by Cp rings between preferred and non-preferred Mo-thioamide diastereomers. Nonetheless, all of the Mo-thioamides examined thus far have their Cp rings oriented (as shown in Fig. 5) with two of the Cp carbons above N and S atoms and with the other Cp carbons staggered with respect to carbonyls. In fact, except for the disordered $CpV(CO)_4$ [33a] and $CpNb(CO)_4$ [33b,c] complexes, all compounds listed in Table VIII have Cp carbons staggered with respect to carbonyls, and eclipsed with respect to some other ligand. The similarities in Cp orientations for a total of *18* structures, crystallizing in *8* space groups, indicate that packing forces cannot be the controlling factor in determining Cp orientations. There appears to be no relationship between the ligand chosen to be eclipsed and the degree of distortion in the two C(O)–M–L *trans* angles. This fact, and the observation that rather bulky groups are eclipsed by Cp carbons, indicate that internal steric interactions are not a major factor in determining Cp orientations.

One interesting feature of the data on Table VIII, is the fact that, in all cases, the ligand eclipsed by Cp in the solid state is one which exerts less of a *trans*-

TABLE IX. Comparison of Cp–Ph and Ph–Ph Interactions.

Compound	Space Group	Inter-Planar Angle (°)	Centroid–Centroid Distance (Å)	Shortest C···H Contact (Å)	Reference
$Cp(CO)_2MoSC(R)NH(R')Ph$					
R = CH_3 R′ = CH_3	$P2_12_12_1$	61.3	4.77	2.89	1
= CH_3 = C_2H_3	$P\bar{1}$	64.7	4.41	2.81	This work
= CH_3 = i-C_3H_7	$P2_1$	58.2	4.48	2.90	5
		59.4	5.31	2.83	
= CH_3 = i-C_3H_7	$P2_1/n$	63.8	4.83	2.83	5
= α-$C_{10}H_7$ = CH_3	$P2_12_12_1$	[98.5][a]	[4.70][a]	[2.66][a]	This work
Benzene I (3 °C–1 atm)	Pbca	84	5.13	2.82	46
Benzene II (–40 °C – 40 kbar)	$P2_1/c$	–	4.38	2.58	47
$(C_6H_6)_2$ (Molecular Beam)	–	–	~5	~3	48

[a] Intermolecular contact between Cp and C(13)–C(18) of α-$C_{10}H_7$.

influence (than carbonyl) amongst the ligands in the base of the square-pyramid. If one accepts that the four ligands in the base may influence each other electronically, then it is not unreasonable that they would also influence bonding to the Cp. What Table VIII shows, is that this electronic influence *is* substantial, overriding any influence arising from angular distortion of the square-pyramid, or from outside packing forces. Table VIII also shows that, for this class of compounds, even a slight modification (through ligand substitution) of an ideal $CpML_4$ structure, leads to an observable preference in Cp orientations. Although rotational barriers have not been measured for any of the compounds on Table VIII, we feel that the barriers should be substantially larger than 0.002 kcal/mol, indicating a need for more accurate, and stereochemically more general, MO calculations on complexes such as $CpML_4$ before any reasonable correlations can be drawn between 'idealized' structures and actual structures.

Before leaving this point, it should be added that the trend shown on Table VIII applies only to *cis*-dicarbonyls, and that even within this class of compounds, there are exceptions: The $CpV(CO)_4$ and $CpNb(CO)_4$ complexes display disordered structures, so far as Cp rings are concerned. Also, square-pyramidal complexes having metal atoms in their basal planes (see ref. 40) show little regularity in their Cp orientations, though they are no more disordered (sterically) than any of the compounds listed in Table VIII. Additional MO calculations on $CpML_4$ complexes, in general may also help explain these exceptions.

Additional structural features of (I)

Both in its central $Cp(CO)_2Mo$ SCN fragment, and in its peripheral groups, compound (I) represents a typical preferred diastereomer of the Mo-thioamide series. The C(8)–C(9) distance (1.509(3) Å) in compound (I) is well within the range of values (1.488–1.511 Å) compiled for the same bond in other Mo-thioamides. The only new structural feature in this compound is the appearance of an ethyl group in the R′ position. Not surprisingly, the (refined) hydrogens of the ethyl group adopt a staggered conformation, with the C(11)–C(18) distance (1.521(4) Å) slightly shorter than that expected for a C–C single bond. This distance, however, is close to the average C–C distance (1.523 Å) reported in the three structures of isopropyl Mo-thioamide derivatives [5]. For a further analysis of individual distances and angles in Mo-thioamide complexes, and for comparison of these compounds to other thioamides, the reader is directed to our first paper on this series of compounds [1].

Additional structural features of (II)

Aside from conformational differences, which will be discussed later, compounds (I) and (II) show great similarities in their central $Cp(CO)_2MoSCN$ fragments, as well as in their optically active amine substituents. In Tables IV and VI, and especially in Fig. 5, one finds similarities not only in bond lengths and angles, but also in torsion angles associated with the optically active substituent groups. Bond distances and angles in the optically active $-CH(CH_3)C_6H_5$ group are identical (to within experimental errors) to those reported earlier for the same substituent in a preferred isomer [1]. The Cp, phenyl, and four-membered Mo–S–C–N rings in (II) are all planar (see Table V), with the largest deviations of atoms from these planes being less than 0.01 Å.

In all respects, the molecular parameters of the α-naphthyl group in (II) corresponds fairly well to

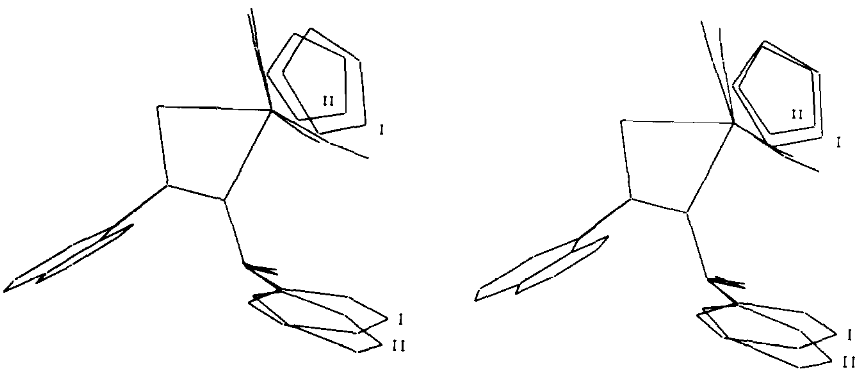

Fig. 6. MFIT stereo view showing similarities between Compounds I and II in the orientation of optically active side groups.

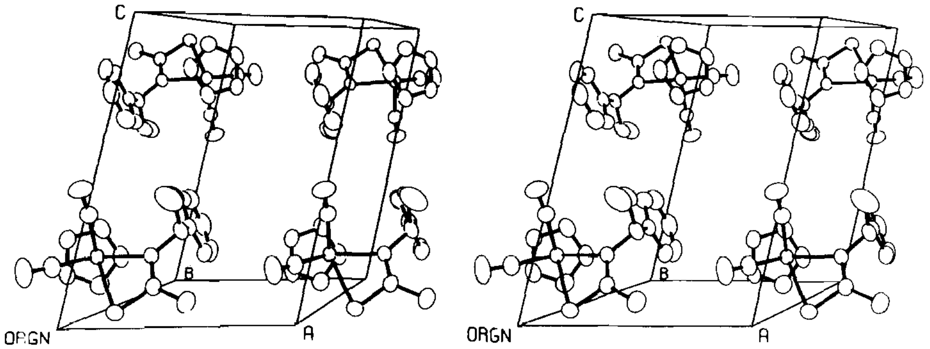

Fig. 7. Stereo view showing the crystal packing in Compound I. Four molecules are depicted to better illustrate the intermolecular contacts.

the same group in α-naphthanoic acid [41] and in 1, 1′-binaphthyl [42]. Around the naphthyl ring, the average C–C distance in the three compounds are: 1.391, 1.404, and 1.389 Å, respectively. In each case, deviations from the average value are small. Across bridgehead carbons [C(13)–C(18)] the distances are: 1.427(4), 1.42(1) and 1.416(3) Å. In all other internal angles, torsional angles, *etc.*, the α-naphthyl group of compound (II) compares favorably with the other two naphthyls. In all three, little or no conjugation is found between the naphthyl rings and the groups substituted at the α-position. The α (C–C) distances for the three compounds are: 1.493(3), 1.46(1), and 1.475(5) Å. Each of these corresponds approximately to the theoretical sp^2–sp^2 single bond distance of 1.477 Å [43]. Furthermore, in all three compounds, the dihedral angles between the planar naphthyl ring and the external conjugated system restrict conjugation across the α-bond. The three dihedral angles are: 97.53°, 11° and 68°. Although both naphthyl and cyclopentadienyl groups lie on the same side of the Mo–S–C–N ring in compound (II), there is no evidence of direct steric interaction between the two groups; the shortest H···H contact between them is approx. 2.8 Å.

Structural differences between (I) and (II)

In Fig. 6, one enantiomer of compound (I) has been chosen for comparison with the correct absolute configuration of compound (II). Best Molecular Fit calculations show the two structures to be almost identical so far as their central Mo–S–C–N fragments are concerned. The major structural difference between the two compounds results from an inversion of chirality at the Mo site: Compound (I) is depicted in Fig. 5, with its Cp group above the MoSCN (ligand) plane, and with its carbonyls projected below the plane. (This can be appreciated best through the use of a stereo viewer). Compound (II), on the other hand, is shown with carbonyls above the ligand plane and with its CP group downward. Minor deviations can also be found in the orientation of the two phenyl groups (on the optically active carbons), probably resulting from the different nonbonding interactions these two groups have with Cp *vs.* carbonyl above the ligand plane.

TABLE X. Selected Non-bonding Contact Distances (Å).

	Atom 1	Atom 2	Symmetry[a] Operation	Translation			Distance[b]
				X	Y	Z	
I	O(1)	H(17C)	1	0	0	0	2.79(6)
	O(2)	H(4)	1	0	0	0	2.73(6)
	O(2)	H(11B)	1	0	0	0	2.78(6)
	O(1)	H(7C)	1	−1	0	0	2.77(6)
	O(2)	H(11B)	2	0	0	1	2.78(5)
	C(12)	H(3)	1	0	0	0	2.84(3)
	C(13)	H(3)	1	0	0	0	2.81(3)
	C(17)	H(3)	1	0	0	0	2.98(3)
	C(18)	H(5)	2	0	0	1	3.39(4)
	C(18)	H(18A)	2	1	−1	1	2.95(4)
II	O(1)	H(3)	2	−1	0	1	2.45(1)
	O(1)	H(17)	2	−1	0	−1	2.79(1)
	O(2)	H(15)	2	0	1	0	2.67(1)
	O(2)	H(11)	2	0	1	1	2.77(1)
	C(15)	H(2)	1	−1	−1	−1	2.88(1)
	C(15)	H(5)	3	1	−1	−1	2.72(1)
	C(16)	H(2)	1	−1	−1	−1	2.85(1)
	C(17)	H(2)	1	−1	−1	−1	2.97(1)
	C(18)	H(19)	1	0	0	0	3.02(3)
	C(20A)	H(17)	1	0	0	0	2.50(3)

[a] Symmetry Operations: 1 – (x, y, z); 2 – (–x, –y, –z); 3 – (½ + x, ½ – y, –z). [b] Distances calculated by program ORFFE [51].

Crystal Packing

Compound (I)

Compound (I) packs in space group $P\bar{1}$, with one molecule in the asymmetric unit. To better illustrate crystal packing, Fig. 7 has been prepared with four molecules (twice the cell contents) shown. From the figure, and from the contact distances listed in Table X, the molecules appear to pack in layers parallel to the (x, y) plane, with their Mo–Cp-(centroid) vectors also parallel to the plane. In Table IIIA, one finds that the fractional coordinates along the z-axis in compound (I) span a range from 0.01 to 0.51, while those for x and y span a much wider range. As a result, there is more interpenetration of functional groups from adjacent molecules, and, on the average, shorter van der Waals contact within the layers (see Table VII). Between layers, the shortest C–H contact (2.95 Å) occurs between atoms (C(1) and H(18A). As already discussed, there are several relatively short intra-molecular C–H contacts between the Cp and phenyl groups, and the intra-molecular Cp(centroid)–Ph(centroid) distance is 4.41 Å. Table VII shows that, in addition to the intra-molecular Cp–Ph contacts, there is a short inter-molecular Cp–Ph contact (5.26 Å) between adjacent molecules; the orientation of the two groups is different, however, indicating that there is no attractive force between them.

Compound II

Figure 8 shows the packing of four symmetry-related molecules in compound (II). The additional symmetry conditions allow for a more uniform packing density than that observed in compound (I). From the figure, it appears that the packing is dominated by contacts between the three types of aromatic groups present in this compound. Although there can be no intra-molecular Cp–Ph contacts in this non-preferred diastereomer (see Fig. 6B and Table X) there are several relatively short inter-molecular contacts between the Cp and carbons C(13) through C(18) of the naphthyl group. The distance between the two centroids (4.70 Å), the interplanar angle (98.5), and the short C–H contacts listed on Table VII are similar to those observed for other complexes (see Table X) where attractive Cp–Ph forces are operative. Thus, these values are typical Cp–Aromatic Ring interactions which seem to be independent of the nature of the aromatic moiety.

Relationship of Structural Parameters to Epimerization Studies

From NMR and polarimetric epimerization studies on 46 square-pyramidal Mo and W-amidinato and -thioamidato complexes, Brunner and coworkers

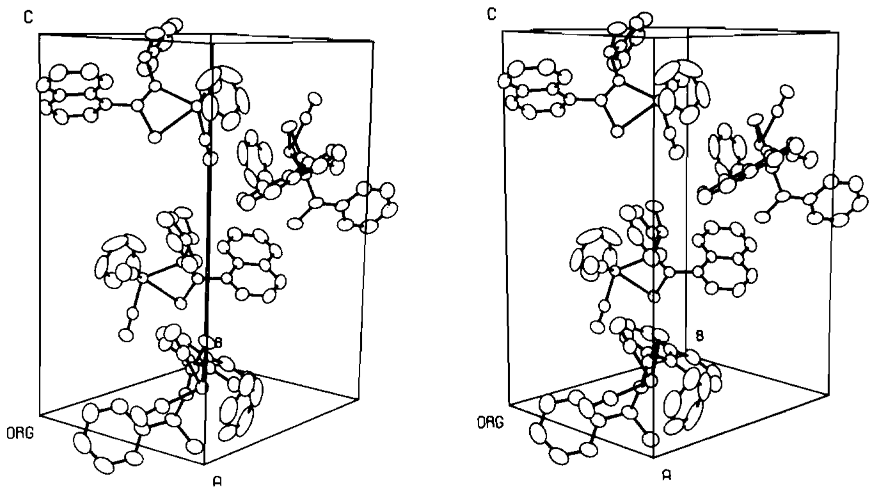

Fig. 8. Stereo view showing the crystal packing in Compound II. Four symmetry related molecules are shown.

[44] have obtained data that are consistent with inversion of chirality at the metal site taking place through a unimolar, metal-centered rearrangement. Though the details of the actual rearrangement mechanism are not known, it is believed to involve a Berry type Pseudo-Rotation [45a] or Turnstile Rotation [45b], using a trigonal-bypyramidal intermediate. In either case, expimerization may be vidualized as taking place through a 180° rotation of the $CpMo(CO)_2$ moiety about some Mo–(Bidentate ligand) vector. It is important to note that in their experiments Brunner and coworkers [44] found equilibrium diastereomeric ratios to be identical to the ratios determined during synthesis. This fact strongly supports the view that the ratios (listed in the Introduction for Mo-thioamides) are the results of conformational energy differences between alternate configurations and are not the result of any external stereo-differentiating conditions present *during synthesis.*

From the diastereomeric ratios listed in the Introduction, it is apparent that steric effects, involving the R and R′ substituents play a major role in determining the relative stabilities for a pair of diastereomers. Although one may imagine any number of interactions that could contribute to the overall conformational energy for a given Mo-thioamide complex, we believe that the relative conformational energies and thus the equilibrium ratio for a pair of diastereomers may be explained on the basis of *three* factors, discussed in what follows, and summarized at the end of this section:

(a) Influence of the exocyclic R groups

Examination of the molecular conformations of compounds (I) and (II) (see Figs. 1 and 3) reveal that the hydrogen on the optically active carbon points directly toward the exocyclic (methyl or α-naphthyl) group and that the C–H vector is nearly parallel to the plane of the Mo–S–C–N ring (the ligand plane). The same orientation of the chiral –CH(R′)Ph group is observed throughout the Mo-thiamide series and also in several unrelated, optically active, Mo complexes we have examined [61b; 34a,b]. In solution, the R substituent has a profound influence on the values of the diastereoisomeric ratios – with R = H, a 50:50 ratio is measured regardless of the substituent R′, and progressively larger R groups lead to pronounced increases in the values of the ratio. In addition to a simple bulk effect, the R group also exerts some electronic influence upon epimerization: With $R' = CH_3$ an $R = C_6H_5$ and p-$C_6H_4OCH_3$, equilibrium diastereomeric ratios of 77:23 and 75:25 are obtained.

In trying to explain the effect of R groups upon epimerization, one is confronted with three problems: first, even in the case of compound (II), with α-naphthyl in the R position, the group is too far removed from any Mo substitutents to exert any *direct* steric influence at the Mo site; second, bonding parameters within MoSCN ligand plane remain remarkably constant throughout the Mo-thioamide series, indicating that the electronic nature of R groups is not a dominating factor in Mo-thioamide bonding; third, although temperature dependent NMR studies yield *total* epimerization energies, the energies for internal motions (*e.g.* rotation of the exocyclic-CH(R′)Ph group) have not been individually determined. For compound (II), for instance, the two epimerization activation energies (starting from pure *P* and *NP* diastereomers) are 19.2(3) and 18.8(3) kcal/mol [10]. These values may be contrasted with the 17.3(3) and 16.8(3) kcal/mol measured [46] for a ligand *conformational* change (with retention of configuration at Mo) in $Cp(CO)_2$-$Mo(NH_2(CO_2CH_3)CH_2S)$. Until more is learned about the energetics of internal motions in Mo-thioamide complexes, very little can be said about the *exact mode* of R group participation during epimerization.

(b) Attractive influence of the phenyl substituent

If all of the steric interactions in the Mo-thioamide series were of repulsive type then one would expect the conformational and configurational differences between *P* and *NP* diastereomers to be caused by (a) a few very short intramolecular contacts (*i.e.* more repulsion) in *NP* isomers or (b) a larger number of short contacts in *NP* isomers. The structures of (I) and (II) (Figs. 1, 3 and Table X) show the contrary to be true: It is the *P* isomers, with (I) as a typical example, that display relatively short non-bonding contacts between their Cp hydrogens and neighboring phenyl carbons. As already documented in our previous paper [5] (and as shown in Table IX– all of our structural investigations of preferred (*P*) Mo-thioamide complexes show the two aromatic groups (Cp on Mo and phenyl, attached to Mo) to be oriented in an edge-to-face arrangement, with an interplanar angle of *ca.* 60° and with centroid-centroid distances of *ca.* 5 Å leading to individual H(Cp)–C(Ph) contacts of just under 3 Å. As Table IX shows, the contacts between Cp and Ph groups in Mo-thioamides are similar to the edge-to-face contacts observed in two crystal modifications of benzene [47a,b]. The Cp–Ph contacts in this series also resemble the intermolecular Ph–Ph associations observed by us [48] and by others [49] in a variety of solid state structures. Although it may be argued that packing forces influence the conformations of molecules and molecular fragments in solid state structures, the chances of having packing forces in crystals belonging to (a) three crystal systems (b) two centrosymmetric space groups ($P\bar{1}$ and $P2_1/c$) and (c) three non-centrosymmetric space groups ($P1$, $P2_1$ and $P2_12_12_1$) all leading to the same basic molecular conformation is a little difficult to believe. Finally, recent molecular beam experiments [50] on dimeric benzene show the $(C_6H_6)_2$ complex to exhibit a T-shaped (C_{2v}) rather than coplanar (C_{6v}) geometry. The presence of T-shaped benzene dimers in the gaseous state make edge-to-face *attractive* interactions in the solid state very reasonable.

Additional indications of attractive Co-phenyl interactions are apparent in the solution NMR data for these and other optically active organometallics. In a recent ^{1}H-NMR study of 46 chiral organometallics [44], including Mo- and W-thioamides Brunner *et al.*, observed the following: 1) In solutions containing pairs of diastereomers, two sharp peaks are observed for protons on freely rotating Cp groups; for compounds (I) and (II) the peak separations are 0.53 ppm and 0.66 ppm, respectively [9, 10]. These peak separations may be compared with the 0.11 ppm observed in a related compound $[(\eta^5\text{-}C_5H_5)(CO)_2MoSC(NCH\text{-}CH_3\text{-}C_6H_5)(\alpha\text{-}C_5H_4N)]$, which exhibits a Cp–Ph (centroid-centroid) distance of 7.93 Å and a diastereomeric ratio of 58:42 [51]. 2) When two peaks are observed, peak integration yields diastereomeric ratios directly 3) In solutions of pure preferred diastereomers, only one peak is observed and it is shifted upfield from the normal H(Cp) region *via* the 'β-phenyl effect'. The upfield H(Cp) shifts observed for preferred isomers are similar to, but no as strong as, those observed by Boekelheide, Mitchell, *et al.* [52, 53] in their studies of hydrogens directed toward aromatic rings in *syn vs. anti* paracyclophanes, metacyclophanes and dithiacyclophanes.

(c) Repulsive influence of the R′ groups

Another contribution to conformational stability and to the values of diastereomeric ratios, in the Mo-thioamide series, results from steric interactions involving the R′ alkyl groups, substituted on the optically active carbons. When one of the substituents on the chiral carbon is aromatic, increase in the bulk of the aliphatic (R′) group leads to increased diastereomeric ratios. When both substituents are aliphatic, however, the ratios are observed [9] to be no greater than 56:44. Thus, bulky aliphatic groups alone *exert* a lesser influence on the values of diastereomeric ratios.

One way in which aliphatic (R′) groups may influence diastereomeric ratios is through repulsive interactions with the Cp and CO groups on Mo. Figure 2B shows that in the non-preferred isomer of compound (II), steric interaction between the methyl and Cp groups is possible. This interaction may be responsible for the deviations in torsion angles around the N–C(1) vector for this compound (see Table VI). By increasing the conformational energy of non-preferred diastereomers, larger R′ groups would increase the overall energy difference between preferred and non-preferred configurations.

Conclusions

The crystal structure of compound (I) is entirely consistent with comments we made earlier [5] regarding the preferred conformations of Mo-thioamides. The appearance of compound (II), the first non-preferred diastereomer has caused us to modify, significantly, our earlier conclusions. Based upon the structural and NMR evidence available thus far, we feel that the conformational stabilities (and thus the equilibrium ratios) for pairs of diastereomers are determined by *specific* intra-molecular non-bonding interactions. Stated as empirical rules, our conclusions are as follows:

Rule 1 – The most significant interaction occurs between the R substituent, and substituents on the optically active carbon. In the solid state, this result in the hydrogen on the β carbon to be directed toward R, close to the ligand (Mo–S–C–N) plane.

Rule 2 – The second major interaction is an attractive force between Cp and phenyl β to Mo. In preferred diastereomers the phenyl will be above the ligand plane, facing the Cp ring.

Rule 3 – In non-preferred diastereomers there is a significant repulsion between the aliphatic R′ group and the Cp. This leads to a slight change in torsion angles about the N–*C vector with hydrogen (on carbon) ending up out of the Mo–S–C–N plane.

References

1 G. M. Reisner, I. Bernal, H. Brunner and J. Wachter, *J. Organometal. Chem., 137,* 329 (1977).

2 H. Brunner, *Acc. Chem. Res., 12,* 50 (1979) and references therein.

3 M. G. Reisner, I. Bernal, H. Brunner and J. Doppelberger, *J. Chem. Soc. Dalton Trans.,* 1664 (1979).

4 G. M. Reisner and I. Bernal, *J. Organometal. Chem., 173,* 53 (1979).

5 G. M. Reisner and I. Bernal, *J. Organometal. Chem.,* in press.

6 $Cp(CO)_2MoN(CH_2Ph)C(Ph)N(S\text{-}CH(CH_3)Ph)$;
a) Preferred isomer ($P\bar{1}$); H. Brunner, G. Agrifaglio, I. Bernal and M. Creswick, *Angew. Chem. Int. Ed. Engl., 19,* 641 (1980); *Angew. Chem., 92,* 645 (1980);
b) Non-preferred isomer ($P2_12_12_1$); I. Bernal, M. Creswick, H. Brunner and G. Agrifoglio, *J. Organometal. Chem., 198,* C4 (1980).

7 R. Kuroda and S. F. Mason, *J. Chem. Soc., Dalton Trans.,* 727 (1979); and references therein.

8 a) H. J. Simpson and R. E. Marsh, *Acta Crystallogr., 20,* 550 (1960);
b) C. Pedone and E. Benedetti, *Acta Crystallogr., Sect. B, 28,* 1970 (1970).
c) E. Benedetti, P. Corradini and C. Pedone, *J. Phys. Chem., 76,* 23 (1972).

9 H. Brunner and R. Lukas, *Chem. Ber., 112,* 2528 (1979).

10 H. Brunner and J. Wachter, *Chem. Ber., 110,* 721 (1977).

11 Instruction Manual, CAD-4 System, Enraf-Nonius, Delft, 1972.

12 X-RAY '72 SYSTEM: crystallographic programs of J. M. Stewart, G. S. Kruger, H. L. Ammon, C. Dickinson and S. R. Hall, University of Maryland, 1972.

13 R. B. Roof Jr., 'A Theoretical Extention of the Reduced Cell Concept in Crystallography', Los Alamos Scientific Laboratory, University of California, 1969.

14 K. A. Kerr and P. J. Ashmore, *Acta Crystallogr., Sect. A, 30,* 176 (1974).

15 J. D. Korp, Program REDUCE, University of Houston, 1975.

16 CAD-4 Operation Manual, Enraf-Nonius, Delft, 1977.

17 M. Creswick, I. Bernal and K. Pannell; submitted for publication.

18 J. D. Korp, Program REDUCE (updated for CAD-4 OS/4 System), University of Houston, 1978.

19 G. M. Sheldrick, 'The SHELX System of Crystallographic Programs', Cambridge University, 1976.

20 Scattering factors for all but Mo were taken from: D. Cromer and J. Mann, *Acta Crystallogr., Sect A, 24,* 321 (1968). Scattering factors for Mo were taken from: 'International Tables for X-ray Crystallography', The Kynoch Press, Birmingham, England, 1974, Vol. IX, p. 100; with anomalous scattering corrections: *ibid.,* p. 150.

21 W. C. Hamilton, *Acta Crystallogr., 18,* 502 (1965).

22 J. M. Bijvoet, A. F. Peerdeman and A. J. van Bommel, *Nature, 168,* 271 (1951).

23 R. S. Cahn, C. Ingold and V. Prelog, *Angew. Chem. Int. Ed. Engl., 5,* 385 (1966); *Angew. Chem., 78,* 423 (1966).

24 K. Stanley and M. C. Baird, *J. Am. Chem. Soc., 97,* 6599 (1976).

25 C. K. Johnson, 'ORTEP-2, A Fortran-Ellipsoid Plot Program for Crystal Structure Illustration', ORNL-5138 Report, Oak Ridge, Tenn., 1972.

26 Outside of this series, thioamides act as unidentate ligands, bonding only through sulfur see: R. L. Girling, J. E. O'Connor and E. L. Amma, *Acta Crystallogr., Sect. B, 28,* 2640 (1972).

27 a) E. M. Shustorovich, M. A. Porai-Koshits and Y. A. Buslaev, *Coord. Chem. Rev., 17,* 1 (1975).
b) T. G. Appleton, H. C. Clark and L. E. Manzer, *Coord. Chem. Rev., 10,* 335 (1973).
c) F. R. Hartley, *Chem. Soc. Rev., 2,* 163 (1973).

28 J. K. Burdett and T. A. Albright, *Inorg. Chem., 18,* 2112 (1979).

29 F. A. Cotton and C. S. Kraihanzel, *J. Am. Chem. Soc., 84,* 4432 (1962);
F. A. Cotton, *Inorg. Chem., 3,* 702 (1964).

30 R. C. Elder, L. Roxanne-Florian, R. E. Lake and A. M. Yacynych, *Inorg. Chem., 12,* 2690 (1937).

31 I. Bernal, G. Reisner and G. Dobson, submitted for publication.

32 G. J. Kruger, G. Gafner, J. P. R. De Villiers, H. Raubenheimer and H. Swanepoel, *J. Organometal. Chem., 187,* 333 (1980).

33 a) J. B. Wilford, A. Whitla and H. M. Powell, *J. Organometal. Chem., 8,* 495 (1967);
b) W. H. Baird, *Ph.D. Thesis,* University of Wisconsin, 1963.
c) I. Bernal, unpublished.
d) S. Chaiwasie and R. H. Fen, *Acta Crystallogr., Sect. B, 24,* 525 (1968).
e) M. J. Bennett and R. Mason, *Proc. Chem. Soc. London,* 273 (1963).
f) M. R. Churchill and J. P. Fennessy, *Inorg. Chem. Soc., 6,* 1213 (1967).
g) J. K. P. Ariyaratne, A. M. Bierrum, M. L. H. Green, M. Ishaq, C, K. Prout and M. G. Swanwick, *J. Chem. Soc. Sect. A,* 1309 (1969).
h) T. N. Sal'nikova, V. G. Andrianov and Yu. T. Struchkov, *Koord. Khim., 2,* 367 (1976).
i) G. A. Jones and L. J. Guggenberger, *Acta Crystallogr., Sect. B, 31,* 900 (1973).
j) G. A. Jones and L. J. Guggenberger, *Acta Crystallogr., Sect B, 31,* 900 (1973).
k) J. R. Knox and C. K. Prout, *Acta Crystallogr., Sect. B, 25,* 1952 (1969).
l) A. T. Liv, W. Beck, G. Huttner and H. Lorenz, *J. Organometal. Chem., 129,* 91 (1977).

34 a) G. M. Reisner, I. Bernal, H. Brunner, M. Muschiol and B. Siebrecht, *J. Chem. Soc. Chem. Commun.,* 691 (1978).
b) G. M. Reisner and I. Bernal, *J. Organometal. Chem., 173,* 53 (1979).

35 Lo-K. Liv, BMFIT computer program, University of Texas Austin, 1977.

36 R. E. Davis and P. E. Riley, *Inorg. Chem., 19,* 674 (1980).

37 T. A. Albright, P. Hoffmann and R. J. Hoffman, *J. Am. Chem. Soc.*, *99*, 7546 (1977) and references therein.

38 a) T. A. Albright, R. Hoffman, Y. Tse and T. D'Ottavio, *J. Am. Chem. Soc.*, *101*, 3812 (1979).
b) T. A. Albright, personal communication.

39 Although librational motion of Cp rings often leads to aberrations in individual C–C and C–M distances, the L–M–Cp(centroid)–C(Cp) torsion angles, calculated for comparison of Cp orientations, are unaffected by librational motion.

40 a) $\mathrm{Hg[CpMo(CO)_3]_2}$: M. M. Mickiewicz, C. L. Raston, A. H. White and S. B. Wild, *Aust. J. Chem.*, *30*, 1685 (1977); Hg is eclipsed.
b) $\mathrm{Ga[CpW(CO)_3]_2}$: A. J. Conway, P. B. Hitchcock and J. D. Smith, *J. Chem. Soc., Dalton Trans.*, 1945 (1975).
c) $\mathrm{Cp(CO)_2Mo(CH_2)_3AsPh_2}$: P. D. Brotherton, C. L. Raston, A. H. White and S. B. Wild, *J. Chem. Soc., Dalton Trans.*, 1193 (1976).
d) $\mathrm{Cp(CO)_3MoMn(CO)_5}$: B. P. Biryukov and Yo. T. Struchkov, *Zh. Strukt. Khim.*, *9*, 655 (1968).
e) $\mathrm{Zn[CpMo(CO)_3]_2}$: J. St. Denis, W. Butler, M. D. Glick and J. P. Oliver, *J. Am. Chem. Soc.*, *96*, 5427 (1974).

41 J. Trotter, *Acta Crystallogr.*, *13*, 732 (1970).

42 K. A. Kerr and J. M. Robertson, *J. Chem. Soc., Sect. B*, 1146 (1969).

43 D. W. J. Cruickshank and R. A. Sparks, *Proc. R. Soc. London, Ser. A*, 270 (1960).

44 H. Brunner, *Acc. Chem. Res.*, *12*, 250 (1979).

45 a) R. S. Berry, *J. Chem. Phys.*, *32*, 933 (1960).
b) I. Ugi, D. Marquarding, H. Klusacek, P. Gillespie and F. Ramirez, *Acc. Chem. Res.*, *4*, 288 (1974).

46 H. Brunner, W. Nowak and D. K. Rastogi, *Inorg. Chim. Acta*, *33*, L115 (1979).

47 a) E. G. Fox, D. W. J. Cruickshank and J. A. S. Smith, *Proc. R. Soc. London, Ser. A*, *247*, 1 (1958).
b) G. J. Piermarini, A. D. Mighell, C. E. Weir and S. Block, *Science*, *165*, 1250 (1969).

48 See crystal packing for (II). Also see crystal packing sections in refs. 5, 6a and 6b.

49 a) T. Sakurai, K. Kobayashi, K. Tsuboyama and S. Tsuboyama, *Acta Crystallogr. Sect B*, *34*, 3465 (1978).
b) H. von Ingartinger and H.-V. Jäger, *Acta Crystallogr. Sect. B*, *34*, 3262 (1978).

50 J. M. Stead, T. A. Dixon and Wm. Klemperer, *J. Chem. Phys.*, *70*, 4940 (1979).

51 H. Brunner and G. Spettel, *J. Organometal. Chem.*, *160*, 149 (1978).

52 R. H. Mitchell and V. Boekelheide, *J. Am. Chem. Soc.*, *96*, 1547 (1974).

53 W. Anker, G. W. Bushnell and R. H. Mitchell, *Can. J. Chem.*, *57*, 3080 (1979) and references therein.

54 IUPAC-IUB Commission on Biological Nomenclature, *J. Mol. Biol.*, *52*, 1 (1970).